Rainfall-runoff processes in urban environments

by

Yihui Chan (N)

Fourth-year undergraduate project

in Group D, 2011/2012

"I hereby declare that, except where specifically indicated, the work submitted herein is my own original work."

Yihui Chan

Date

CONTENT

Technical Abstract

The study of the relationship between rainfall and runoff is increasingly important today due to increasing urbanization and hence the need for urban planning and proper design of drainage systems to prevent flooding. This project will investigate the relationship between rainfall and runoff in an urban environment as well as the influence of buildings on the relationship using an in-house computer model. Factors investigated include the building layout, the terrain slope and the building density. As an urbanized area receives a significant proportion of its surface runoff from spatially distributed direct precipitation over the area, the numerical model used in this study allows a direct transformation of spatially distributed rainfall into surface runoff.

The numerical model used is the Total Variation Diminishing (TVD)-MacCormack scheme that solves the shallow water equations (SWE) by Liang et al. (2006). The depth averaged two dimensional (2D) -SWE solved by the model consists of 3 partial differential equations concerning mass and momentum conservation. Surface runoff is very shallow as compared to the length of the region under study and the use of a 2D model in this application is hence valid.

The numerical model is validated by reproducing analytical results and experiments conducted by Iwagaki (1955), Gottardi & Venutelli (2008), Cea et al. (2008) and Cea et al. (2009). Simulation results compared very well with the published results and highlighted issues that might be important in future simulations. Firstly, simulations based on Iwagaki (1955) indicated the need to specify the Manning's roughness coefficient accurately. Secondly, simulations based on Gottardi & Venutelli (2008) indicated the potential problems associated with very small slopes. Lastly, simulations based on Cea et al. (2009) showed the importance of defining the domain topography accurately. It was also noted during tests that the numerical domain had to be extended to generate rapid flows at the downstream boundary, so as to reproduce the effect of the sudden ground level decrease at the catchment outlet in physical experiments.

Three methods of representing buildings were considered in validation tests based on Cea et al. (2009). These were namely the Building-Hole (BH), Building-Block (BB) and Increased-Roughness (IR) methods. The BH method involved representing obstructions as holes in the numerical domain such that any rainfall on the buildings is ignored. It is hence necessary to artificially increase the rainfall intensity to maintain the required discharge. The BB method

includes the buildings in the numerical mesh as elevated ground. Lastly, the IR method involves increasing the bed friction coefficient of the areas occupied by buildings to a significantly larger value compared to the surrounding surfaces. The BH method provided the best balance of numerical stability and accuracy and was chosen to represent buildings in subsequent simulations.

The numerical model was applied in parametric studies of the effect of building layout, building density and terrain slopes on the surface runoff in an urban setting. Seventy eight simulations were carried out based on 6 building layouts, 3 rainfall discharges, 4 rainfall durations and 4 terrain slopes. The building layouts-Y20, Y12, X20, X12, S20 and S12 and 3 rainfall discharges of 7, 15 and 25 l/min were based on Cea et al. (2009). In addition, rainfall duration of 10, 20, 40 and 60s and four slopes of 0.5%, 1%, 3% and 5% were considered.

Firstly, discharge was generally largest when buildings were aligned with their length parallel to the flow direction. More complicated layouts provided greater obstruction and reduced the rate of discharge out of the domain, resulting in potential flooding in real scenarios. The influence of layout was however affected by the rainfall intensity imposed and potential problems in the simulation associated with steep slopes and rapid flows were noted and should be considered in future simulations. Secondly, larger terrain slopes generally produced hydrographs with shorter time of concentration and larger peak discharges. The simulations indicate that general flooding can occur in urban settings with small slopes as water dissipates slowly. Also, localised flooding and high velocity flows are possible in areas with large slopes as water rush towards the domain outlet. Lastly, a lower building density was found to reduce the time of concentration and increase the peak discharge. However, the significance was also influenced by the building layout and rainfall intensity imposed.

The simulations carried out have shown the capability and potential of the numerical method in modelling surface runoff from direct precipitation in urban areas. The simplified representations of urban settings provide a strong foundation for understanding how building layout, building density and terrain slope affect the surface runoff characteristics. These can be developed by considering a larger range of factors including building shapes and surface roughness and would provide a useful tool for the design of drainage systems in new and existing urban developments.

1. Introduction

1.1 Background

The study of the relationship between rainfall and runoff is increasingly important today due to increasing urbanization and hence the need for urban planning and proper design of drainage systems to prevent flooding. Advances in numerical analysis has allowed the simulation of two-dimensional shallow water flow as is the case in urban rainfall-runoff processes, and allows for a future in real-time flood prediction in towns and cities. This project will investigate the relationship between rainfall and runoff in an urban environment as well as the influence of buildings on the relationship using an in-house computer model.

According to the United Nations Department of Economics and Social Affairs, urban populations are expected to increase from 745.5 million in 1950 to 3.6 billion today and an estimated 6.3 billion in 2050. Urbanization causes changes to the physical environment and affects the way in which precipitation is drained. For example, surfaces are paved and made impervious, hence reducing the infiltration of rainfall into the soil and increasing surface runoff. Peak discharge in an urbanized area thus increases and occurs much quicker as compared to a rural or suburban area, increasing the risk of flooding if adequate drainage systems are not in place. Presence of buildings and changes to the terrain will also affect the water flow pattern and these will be investigated in this project.

1.2 Previous researches

In many studies of flooding and inundation previously, it is usual to impose a discharge hydrograph at a location upstream of the region in study. This discharge hydrograph is usually calculated from a hydrological model that considers the "precipitation intensity, catchment surface, mean slope and soil" type (Cea et al, 2008). This is acceptable when the input water discharge is "generated mostly upstream from the area of study and therefore, there are no significant changes in the water discharge over the region of interest" (Cea et al, 2009) such as in the downstream section of a river. For an urbanized area however, this method is unacceptable as it receives a significant proportion of its surface runoff from spatially distributed direct precipitation over the area. The numerical model used in this study allows a direct transformation of spatially distributed rainfall into surface runoff and the input into the model is the rainfall intensity.

Some previous studies have been reported in the literature. Iwagaki (1955) provided one of the initial physical experiments simulating rainfall-runoff processes in a laboratory slope involving 3 different slopes of 8m length, each subjected to a different rainfall intensity. Gottardi and Venutelli (2008) used 2 different numerical models and compared 1D and 2D numerical results obtained with both analytical and experimental results by Morgali and Linsley (1965) and Govindaraju et al. (1990). Cea et al. (2008) conducted a preliminary experiment involving 2 walls on a 3 slope terrain in a rainfall simulator. Subsequently, Cea et al. (2009) conducted 72 experiments in "several simplified laboratory configuration of urban catchments" using the same model which involved 8 catchment configurations and 9 input hyetographs. The model used to simulate the terrain consisted of 3 stainless steel planes of 0.05 slope and the output hydrograph was measured and compared to numerical simulations. To validate the TVD-MacCormack scheme used in this project in simulating 1D and 2D shallow water flows, comparison of the numerical results obtained were made against the published analytical and experimental results by the above authors. In addition, the validation tests help provide an understanding of the numerical model and features that need to be considered in the input model to ensure accurate results.

1.3 Present study

Parametric study is carried out to study the effects of various factors on the rainfall-runoff processes in an urban environment and to present the numerical model's capability as a tool in rainfall-runoff modelling applications. Factors studied in this project include the layout of the buildings, the building density and the slope of the terrain. A total of 78 simulations were carried out to include the 3 layouts, 2 building densities, 4 slopes, 3 rainfall discharges and 4 rainfall durations in various combinations. Other factors that can be investigated include the terrain roughness and building shape. The current model is a simplified representation of an urban environment which would otherwise include features such as drains, underground sewers, roads and parks which would affect the removal of water from the surface. Although the tool neglects such features, it contributes towards the understanding of how building layout, density and slope affect surface runoff, and provides a strong foundation for future modelling of urban surface runoff that can includes a larger variety of urban features.

The numerical model used in this project is the Total Variation Diminishing (TVD)-MacCormack scheme that solves the shallow water equations (SWE) by Liang et al. (2006). The depth averaged two-dimensional (2D) -SWE solved by the model consists of 3 partial differential equations concerning mass and momentum conservation. Surface runoff in urban areas is very shallow as compared to the length of the region under study and hence the use of a 2D model in this application is valid. A three-dimensional (3D) model of an urban environment is not practical today due to "the computation cost and the field data needed to build a detailed 3D model of an urban region" (Cea et al, 2009). Although this prevents the analysis of rain falling onto the rooftop of buildings and their impact on the surface runoff, their effects are assumed to be negligible as the aim is to investigate the effect of building layout, density and terrain slope on the surface runoff.

2. Numerical Model

2.1 Shallow water equations and Total Variation Diminishing-MacCormack scheme

The numerical model used in this project is the TVD-MacCormack scheme as proposed by Liang et al. (2006). The model is capable of solving the SWE efficiently and was validated against hypothetical and experimental dam break scenarios in previous papers. The details of the model will not be discussed in this paper. However, a general description will be provided and further details of the mathematical model and results from previous validation tests can be found in Liang et al. (2006).

The 2D-SWE "are a system of three partial differential equations with three unknowns which are defined over a 2D spatial domain" (Cea et al, 2008). Ignoring the effects of Coriolis acceleration, wind and viscous forces, the general form of the SWE can be written as

$$\frac{\partial \eta}{\partial t} + \frac{\partial q_x}{\partial x} + \frac{\partial q_y}{\partial y} = 0 \tag{1}$$

$$\frac{\partial q_x}{\partial x} + \frac{\partial\left(\frac{\beta q_x^2}{H}\right)}{\partial x} + \frac{\partial\left(\frac{\beta q_x q_y}{H}\right)}{\partial y} = -gH\frac{\partial \eta}{\partial x} - \frac{g q_x\sqrt{q_x^2+q_y^2}}{H^2 C^2} \tag{2}$$

$$\frac{\partial q_y}{\partial y}+\frac{\partial\left(\frac{\beta q_x q_y}{H}\right)}{\partial x}+\frac{\partial\left(\frac{\beta q_y^2}{H}\right)}{\partial y}=-gH\frac{\partial\eta}{\partial y}-\frac{g q_y\sqrt{q_x^2+q_y^2}}{H^2C^2} \quad (3)$$

"where t is the time; η is the water surface elevation above the datum; q_x and q_y are the discharge per unit width components in the x and y directions, respectively; β is the correction factor for the non-uniform vertical profile velocity profile, which equates to 1.0 for a uniform velocity distribution and 1.016 for a seventh power law velocity distribution; H = h + η is the total water column depth, with h being the water depth below datum; g is the acceleration due to gravity; and C is the Chezy roughness value" (Liang et al, 2006).

To ensure stability in the simulation, the maximum time step is restricted by the Courant-Friedrich-Lewy (CFL) condition.

$$\Delta t \leq \frac{\Delta x}{\max\left(\frac{\sqrt{q_x^2+q_y^2}}{H}+\sqrt{gH}\right)} \quad (4)$$

where Δt is the time step used in the computations; Δx is the grid size; q_x and q_y are the velocity in the x and y direction respsectively; H is the total water depth and g is the gravitational acceleration.

2.2 Methods of representing buildings

The buildings and obstructions examined in the simulations are incorporated into the terrain as elevated ground with the elevations corresponding to the heights of the buildings or obstructions. This is physically similar to the Building-Block (BB) method described in Cea et al. (2009). However, it is more similar to the Building-Hole (BH) approach by Cea et al. (2009) in the numerical simulation as rainfall on the buildings and obstructions are ignored in the calculations. Hence, it may be necessary to artificially increase the rainfall intensity to account for the loss. A third method of representing buildings involves increasing the surface roughness of the areas occupied by the buildings significantly. These 3 methods will be discussed in section 3.4.2.

The effects of bed friction, bed slope and precipitation had been considered in this model. However, infiltration, evapotranspiration, interception and retention had been ignored as they are assumed to be insignificant in the scenarios that will be analysed. For example, ground surfaces in urban areas are often paved and hence infiltration will be limited. Although parks and open fields exist in urban areas and have significant infiltration, these areas are not considered in the analysis. Evapotranspiration is also ignored due to the nature of the rainfalls analysed which are very short, providing no time for evapotranspiration to occur. The only parameter that needs to be determined is the bed friction coefficient that can be represented by Manning's or Chezy's coefficient. In addition, small scale microtopography is not considered separately in the model, but its effect is included within the bed friction coefficient (Cea et al, 2008).

3. Model Validation

The numerical model is validated by reproducing analytical results and experiments conducted by Iwagaki (1955), Gottardi & Venutelli (2008), Cea et al. (2008) and Cea et al. (2009). Validation was conducted on both 1D and 2D geometries and results from the validation tests will be presented. The first validation test compares the simulation results with 3 series of analytical and experimental results presented in Gottardi & Venutelli (2008).The second test model the 1D experiments conducted by Iwagaki (1955) in which the output hydrograph is measured for a three-slope terrain with correspondingly different rainfall intensities for each slope. 2D validation tests were conducted based on physical experiments by Cea et al. (2008) and Cea et al. (2009). The 2 series of experiments were conducted on a terrain consisting of 3 slopes forming a valley. In the first series, 2 walls were built on the slopes to channel the water into the centre of the terrain, hence increasing the time of concentration and length of the outlet hydrograph. In Cea et al. (2009), buildings in 8 different configurations were built onto the slope and subjected to rainfall represented by 9 hyetographs, producing 72 experiments. The 9 hyetographs were derived from 3 rainfall discharges of 7, 15 and 25 l/min and 3 durations of 20, 40 and 60s. In the validation test, only the X20 and Y20 layouts were modelled as their results had been published and they provided good opportunities for understanding the numerical model.

Three methods of representing buildings were used in the validation tests involving results from Cea et al. (2009). They will be compared to determine the best method for representing buildings in subsequent simulations. The comparison of simulation and experiment results also showed the key features associated with each building representation method which can be considered in future simulations. The 4 series of validation tests will be discussed in this section.

3.1 Gottardi & Venutelli (2008)

Gottardi & Venutelli (2008) compared simulation results using 2 numerical models with analytical results of a hypothetical rainfall, experimental results from Morgali and Linsley (1965) and results using the Saint-Venant equations by Govindaraju et al. (1990). A total of 6 1D simulations were presented in Gottardi & Venutelli (2008) and reproduced using the in-house computer model. Comparison of the simulation and published results are presented.

3.1.1 Hypothetical rainfall

A hypothetical simulation was carried out to model one-dimensional (1D) flow along an inclined plane. The model consists of a slope of length L = 200m, unit width, gradient S_0 = 0.001 and Manning's roughness coefficient n_m = 0.03$m^{-1/3}$s. A rainfall intensity of r = 60mm/h was imposed for t = 1h. For the numerical model, a domain size of length 210m, grid size Δx = 5m, time step Δt = 7s and total simulation time of 6500s was used. The extended domain length of 210m was used instead of 200m as the edges of the domain are ignored in the simulation. Hence, the rainfall on the edges are ignored and the domain must be extended to maintain the correct discharge. The simulation and analytical results are shown in Figure 1.

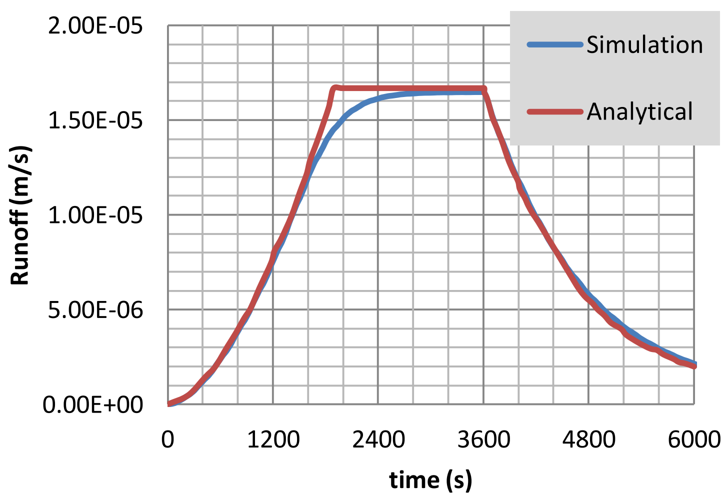

***Figure 1**:Runoff generated by hypothetical rainfall in Gottardi & Venutelli (2008)*

As seen in Figure 1, the simulation results compare reasonably well with the analytical results. The peak runoffs are very similar at approximately 1.68x10^{-5} m/s and the falling limb corresponds very well. Slight differences exist with regards to the rising limb and the time of concentration, with the analytical results showing t_c = 1900s and the simulation producing t_c = 2800s approximately.

3.1.2 Morgali & Linsley (1965)

Gottardi & Venutelli (2008) compared simulation results with analytical solutions and experimental results obtained by Morgali & Linsley (1965). The experimental domain is a turf plane of length L = 21.945m and slope S_0 = 0.04. 2 experiments were carried out. In the first case, a uniform rainfall intensity of r = 2.58233x10^{-5} m/s was imposed on the slope of Manning's coefficient n_m = 0.5$m^{-1/3}$s. In the second case, a uniform rainfall of r = 1.33350 x 10^{-5} m/s was imposed with n_m = 0.4$m^{-1/3}$s. For both cases, the simulation domain was 22.5m long to account for the ignored edges. The grid size and time step used were Δx = 0.25m and Δt = 0.5s respectively. As no rainfall duration was suggested and steady state where the runoff remains constant had been achieved, a rainfall duration of T=1200s which is longer than the time of concentration was imposed.

The analytical, experimental and simulation runoff hydrographs obtained for the 2 cases are shown in Figure 2(a,b) respectively.

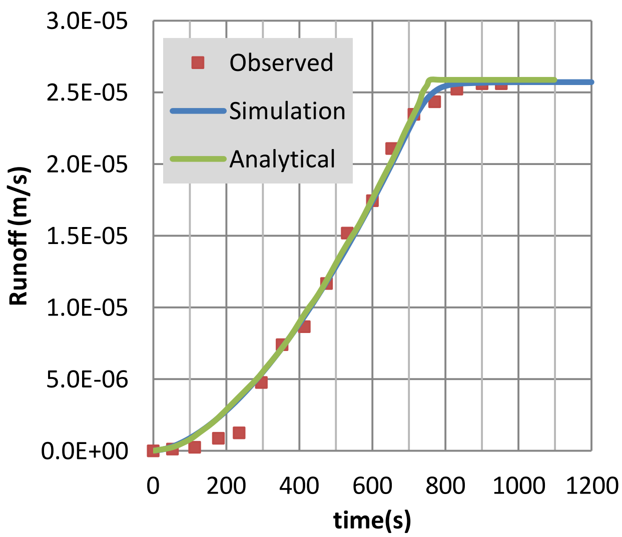

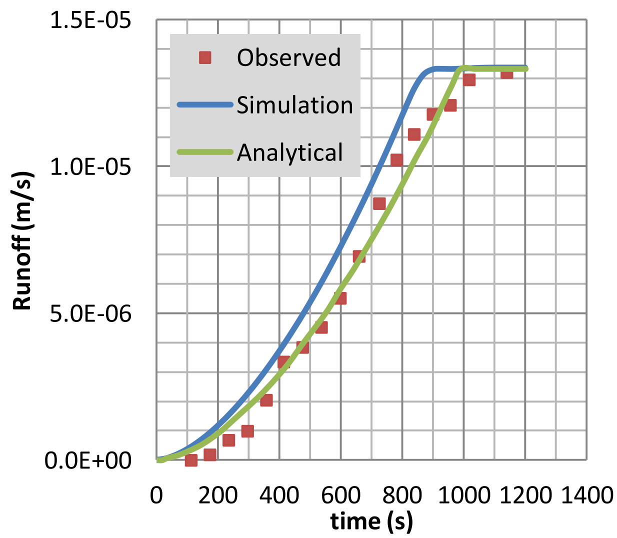

***Figure 2(a,b)**: Results of Case 1 and Case 2 in Morgali & Linsley (1965)*

In the first case, the simulation results correspond very well with both the analytical and experimental results. The slower experimental flow initially could be due to interference by the grass or rainwater being absorbed by the ground (Gottardi & Venutelli, 2008). A similar discrepancy is observed in the simulation carried out by Gottardi & Venutelli (2008).

The simulation result obtained in the second case is less accurate than in the first case, with much faster flow compared to both the analytical and experimental results. This may be due to the smaller discharge, smaller water depth, and the dependence of Manning's roughness coefficient on the flow Reynolds number. Manning's formula assumes that the flow is in the rough turbulent flow regime. However, the flow is laminar when it is very shallow and slow, and technically, the formula should not be used. Although the time of concentration is lower in the simulation, the peak runoff is the same across the 3 results.

3.1.3 Govindaraju, Kavvas & Jones (1990), Changing rainfall intensity in time

Govindaraju et al. (1990) considered 3 cases in which the rainfall intensity was uniform over the entire domain but changes in time. The plane considered has a length L = 21.945m and the value of Chezy roughness coefficient C_c, slope S_0 and input rainfall for each of the 3 cases are tabulated in Table 1.

***Table 1**: Values of C_c, S_0 and rainfall for Cases (a),(b),(c) in Govindaraju et al. (1990)*

Case	Chezy coefficient, C_c ($m^{1/2}/s$)	Slope, S_0	Time, t(s)	Rainfall, r (m/s x 10^{-5})
a	1.336	0.001	$0 \le t \le 600$	2.82222
			$600 < t \le 1200$	1.41111
			$1200 < t \le 1800$	2.82222
			$1800 < t \le 2400$	1.41111
			$t > 2400$	0
b	1.767	0.04	$0 \le t \le 600$	1.41111
			$600 < t \le 1200$	2.82222
			$1200 < t \le 1800$	1.41111
			$1800 < t \le 2400$	2.82222
			$t > 2400$	0
c	1.767	0.04	$0 \le t \le 600$	2.82222
			$600 < t \le 1200$	1.41111
			$1200 < t \le 1800$	2.82222
			$1800 < t \le 2400$	1.41111
			$t > 2400$	0

L = 22m was used in the simulations with a grid size Δx = 0.25m and time step Δt = 0.5s.

The hydrographs obtained from the 3 cases are shown in Figure 3(a,b,c) respectively. Overall, simulation results compare very well with the analytical results using the Saint-Venant equations for cases (b) and (c), especially in matching the peak runoff and changes in gradient. The lower peak runoff observed for case (a) was also seen in Gottardi & Venutelli (2008). This is possibly due to inaccuracies in setting up the very small slope in the experiment.

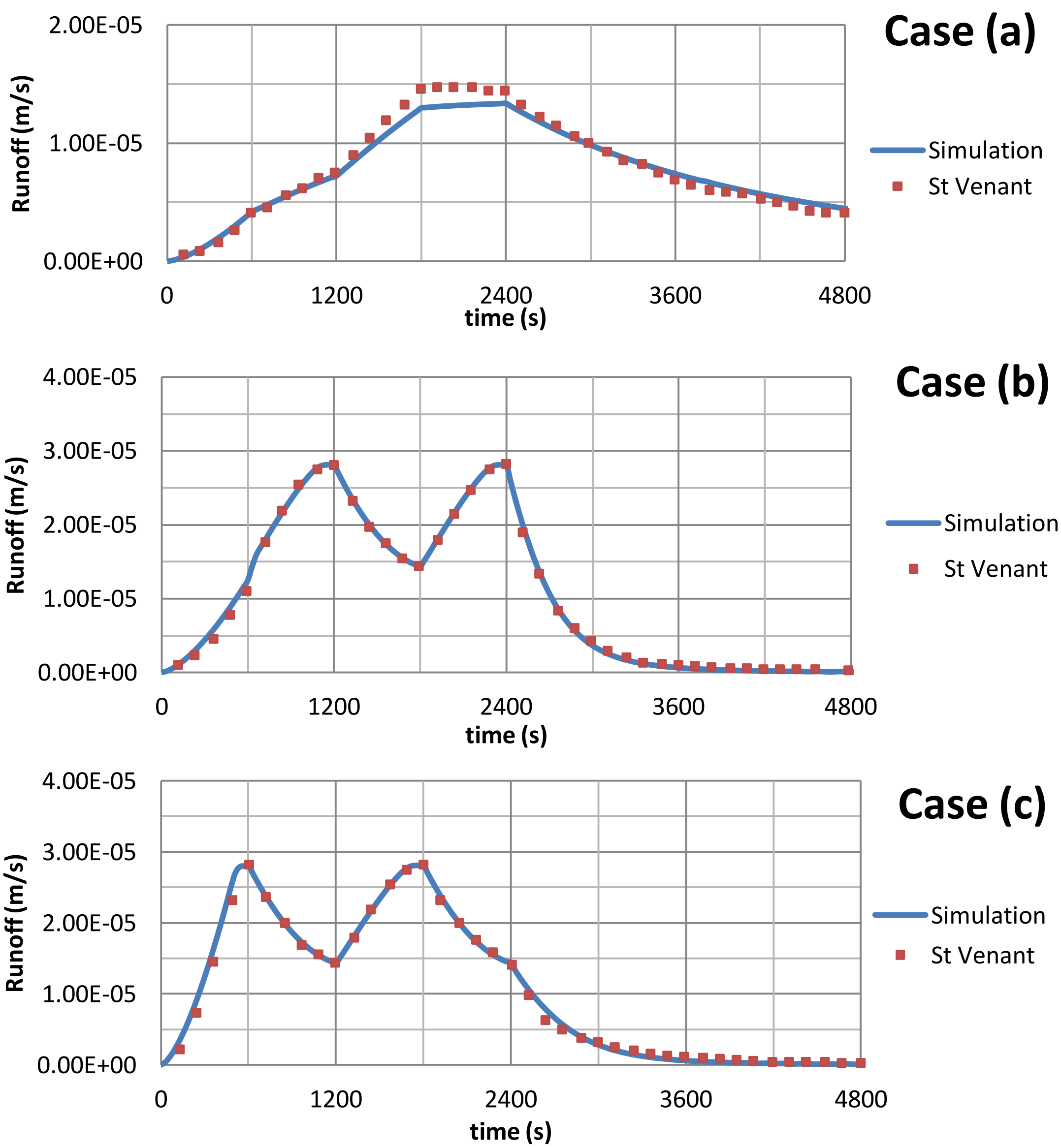

Figure 3(a,b,c)*: Results of Cases (a),(b),(C) in Govindaraju et al. (1990)*

3.2 Iwagaki (1955)

Iwagaki (1955) conducted experiments with a 24m smooth aluminium terrain consisting of 3 planes of equal length. Each 8m plane had a slope of 0.02,

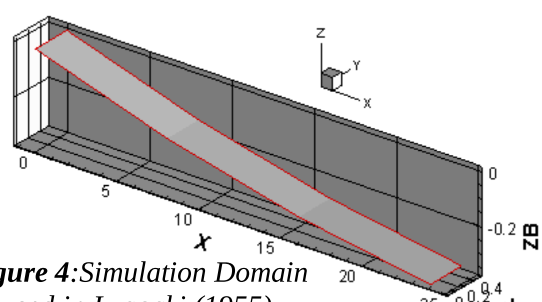

Figure 4*:Simulation Domain used in Iwagaki (1955)*

0.015 and 0.01 and rainfall intensity of 3920, 2300 and 2880mm/h from upstream to downstream respectively. 3 different experiments with rainfall duration of 10, 20 and 30s were conducted. In Cea et al. (2008), the bed friction coefficient was calibrated using the experimental results from Case 1 and the Manning's coefficient was set as n_m = 0.009$m^{-1/3}$s. This value was used in simulating all 3 cases in Cea et al. (2008) and was used in this project's numerical model. The time step used was Δt = 0.05s and the grid size Δx = 0.25m. The simulation domain is shown in Figure 4.The results are shown in Figure 5(a,b,c).

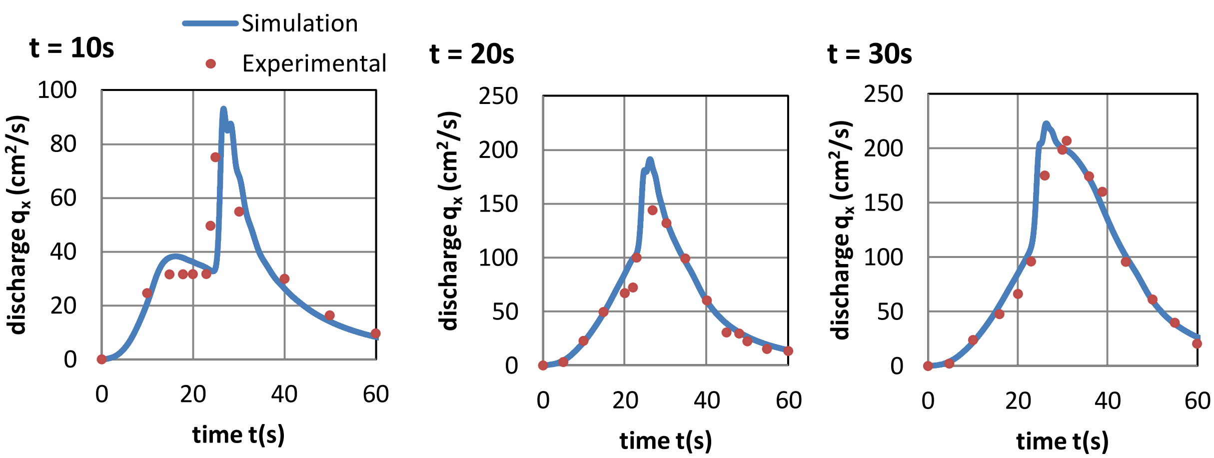

Figure 5(a,b,c): *Results of Cases 1,2,3 in Iwagaki (1955)*

The simulation overestimates the peak discharge especially for Case 1 and 2 in which the durations of the rainfall t = 10 and 20s respectively. In Cea et al. (2008), it was noted that "a too low value of Manning coefficient overestimates noticeably the peak discharge". A value of n_m=0.008$m^{-1/3}$s used in their simulation for Case 1 is shown to produce similar results to this project's simulation. Since the bed friction coefficient had been calibrated to match the experimental and numerical results, a larger value of Manning's coefficient could be used to re-run the simulations. However, the overall shapes of the graphs have matched very well.

3.3 Cea et al. (2008)

Cea et al. (2008) conducted physical experiments to study the shallow water flow "generated by a uniform rainfall over a simple 2D geometry". The model consists of 3 stainless steel planes of 0.05 slope that form a channel in a 2 x 2.5m rectangular basin. Rainfall is provided using a grid of 100 uniformly distributed nozzles over the entire basin and the hydrograph at the system outlet is measured. Three scenarios with differing rainfall intensities were investigated. In the first case, a rainfall intensity of 317mm/h was applied for 45s. In the second case, an intensity of 320mm/h was applied for 25s, stopped for 4s, and reapplied for another 25s. In the last case, an intensity of 328mm/h was applied for 25s, stopped for 7s before being reapplied for another 25s. Figure 6 shows a diagram of the slope used in this experiment.

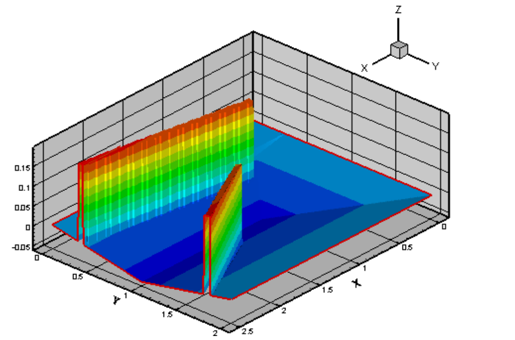

Figure 6*: Study Domain in Cea et al. (2008)*

Cea et al. (2008) expected a few problems that may cause disparities between the simulation and experimental results. Firstly, the rainfall intensity provided by the nozzles may not be uniformly distributed. Secondly, surface tension which prevents water movement when the water depth is too shallow needs to be removed or reduced. Thirdly, the nozzles may continue to leak even after the rain is stopped. Lastly, a small time lag occurs during the start of the experiments when the rainfall intensity increases from zero to the maximum value. These problems are not considered in the numerical model but should be considered when analyzing the numerical and experimental results.

In the simulations, a numerical mesh of 50451 elements and element size 1cm^2 was used to represent the surface area of 5m^2. The grid ranged from 1 to 251 in the x-direction and 1 to 201 in the y-direction to represent a value of 0 to 250cm and 0 to 200cm respectively. The numerical mesh used is shown in Figure 7. In this series of simulations, the elements representing the walls and boundaries of the domain are excluded in the calculations. Any rain falling on these elements are hence ignored in the simulations. This method is equivalent to the Building-Hole method set out in Cea et al. (2009). The loss of rainfall using this method is however insignificant in this case as the area occupied by the walls and edges is very small. Hence, the rainfall intensity had not been artificially increased.

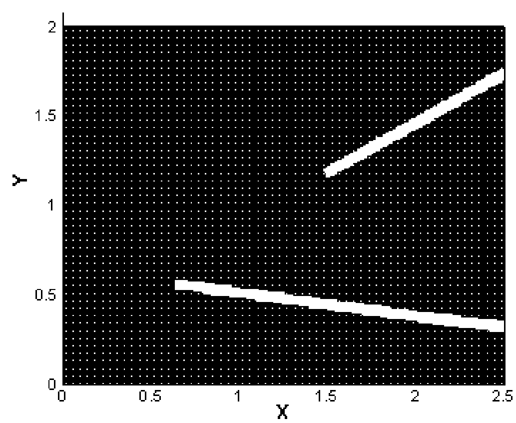

Figure 7*: Computational Mesh for the case in Cea et al. (2008)*

The output hydrographs from the simulations and experiments for all 3 cases are shown in Figure 8(a,b,c). The corresponding hyetographs are shown in Figure 8(d,e,f).

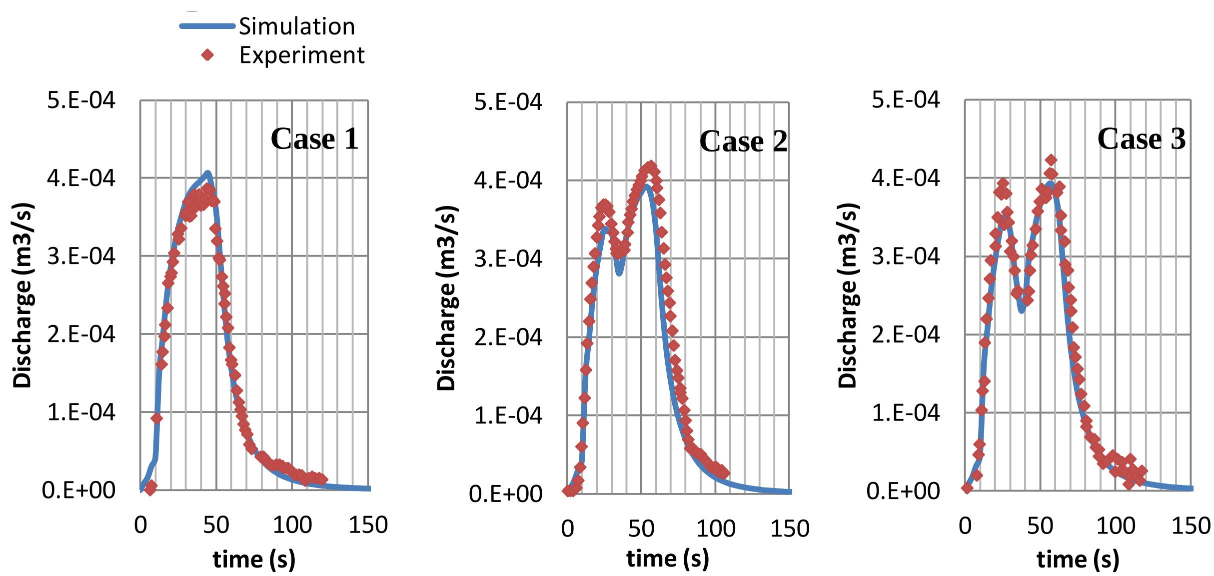

Figure 8(a,b,c):*Hydrographs of Cases 1,2,3 in Cea et al. (2008)*

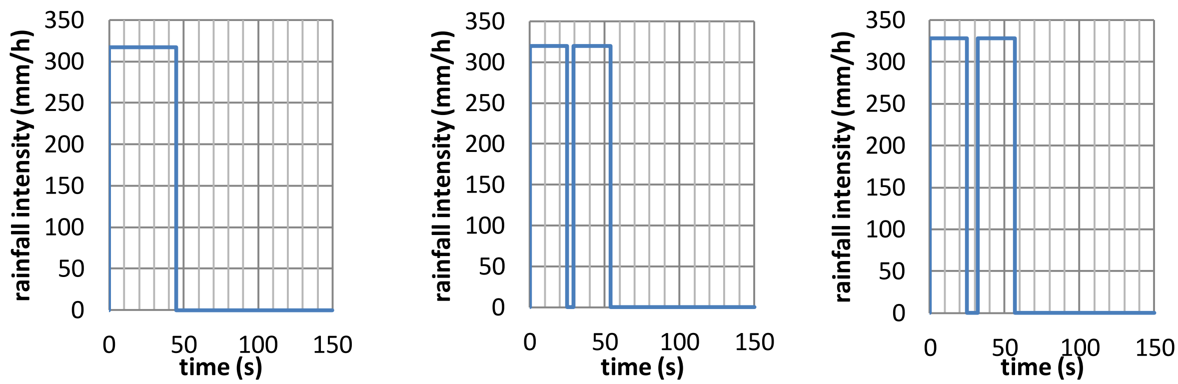

Figure 8(d,e,f): *Hyetographs for Cases 1,2,3 in Cea et al. (2008)*

Overall, the agreement between the experimental and simulation results have been satisfactory considering the potential problems in the experiments as mentioned above. Although the peaks of the hydrographs are overestimated in Case 1 and underestimated in Case 2 and 3, the shapes of the hydrographs have been very well predicted overall.

Simulations carried out by Cea et al. (2008) produced similar results and a few features were noted. Firstly, the slight overestimation of the discharge in the first few seconds of the simulation is due to the time taken for the discharge from the nozzles to increase from zero to a constant value during the experiment. Secondly, the simulation underestimates the tail of the hydrograph and this is likely due to water leaking from the nozzles after the rainfall has ceased. This volume of water is not considered in the numerical simulation and contributes to increasing the output hydrograph in the experiment. Thirdly, the discharge increases until the rainfall is stopped at 25s and decreases immediately thereafter in Cases 2 and 3. When the rainfall is restarted after 4s and 7s respectively, the discharge continues to decrease for a few seconds before increasing again. This is due to the time needed before all the rain falling on the slope reaches the outlet and contribute to the hydrographs.

3.4 Cea et al. (2009)

The fourth series of validation tests is based on Cea et al. (2009). The authors conducted 72 physical experiments in a rainfall simulator based on “8 simplified layouts of buildings in an urban catchment” (Cea et al, 2009) and 9 hyetographs. The experiment results were used to validate the authors’ numerical model which involved 2 methods of representing buildings, namely the Building-Hole and Building-Block method. To validate the numerical model used in this project, 25 simulations involving the Y20 and X20 building layouts, 25 l/min input rainfall discharge, rainfall duration of 20, 40 and 60s as well as 3 methods of representing the buildings were carried out. The 3 methods of representing buildings are namely the Building-Block(BB), the Building-Hole(BH) and the Increased-Roughness(IR) methods. The BH method was found to be most effective overall and will be used in the parametric study subsequently. The description of the experimental set-up, the numerical model used and the results of the validation tests are presented in this section.

3.4.1 Experimental set-up

Using the same slope as in Cea et al. (2008), Cea et al. (2009) conducted 72 physical experiments to model the 8 building layouts under 9 hyetographs. The 9 hyetographs were derived from spatially uniformly distributed rainfall intensities based on discharges of 7, 15 and 25 l/min and durations of 20, 40 and 60s. The hyetographs imposed are representative of extreme precipitation events that are characterized by high intensity rainfall and short duration. The durations used were also determined by the concentration time of the experiments, which depend on the size of the experimental domain, the building configurations and the rainfall intensity that was imposed. The buildings in each of the 8 layouts were represented by blocks in the physical experiment. Each building was 30 x 20cm in plan and 20cm high. The slopes of the roofs were 45°. Figure 9 and Table 2 show the 8 urban building layouts and hyetographs used in the experiment respectively.

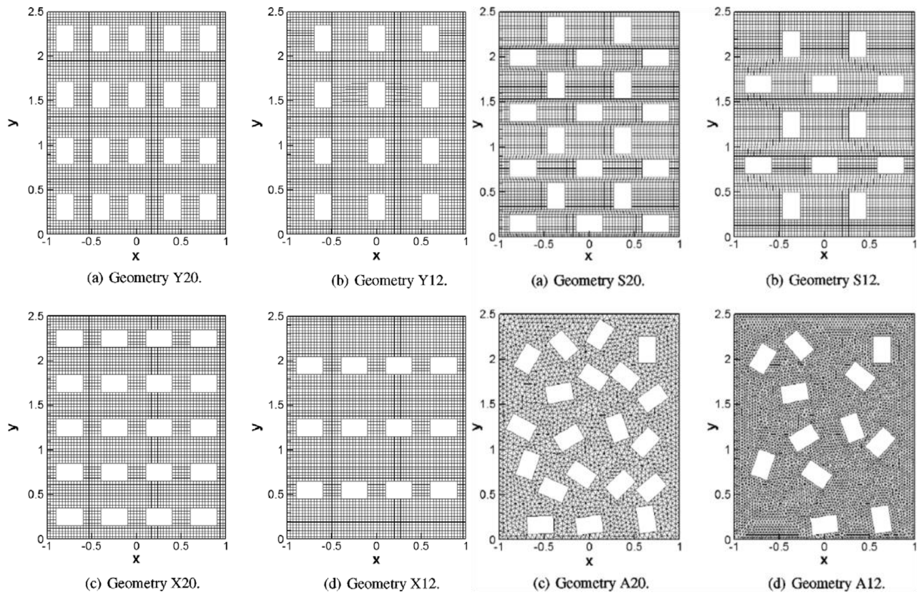

Figure 9*: 8 Urban Building Layouts used in Cea et al. (2009)*

<u>***Table 2****: Cea et al. (2009) Hyetographs*</u>

Hyetograph	Rainfall Discharge (l/min)	Rainfall Intensity (mm/h)	Rainfall Duration (s)
Q7T20	7	84	20
Q7T40	7	84	40
Q7T60	7	84	60
Q15T20	15	180	20
Q15T40	15	180	40
Q15T60	15	180	60
Q25T20	25	300	20
Q25T40	25	300	40
Q25T60	25	300	60

As mentioned in the case of Cea et al. (2008), a few challenges may cause uncertainties in the experiments.

Firstly, the rainfall may not be spatially uniform due to minute differences in the discharges from the nozzles and their orientation. A sensitivity analysis was carried out in Cea et al. (2009) to examine the effect of variations in the spatial distribution of the rainfall intensity on the outlet hydrograph. The effect was found to be negligible. The global experimental uncertainty is defined as the "difference between the discharge imposed for each experiment and the discharge calculated from the volume of water collected at the end of the experiment" (Cea et al, 2009). This was found to be around 5% in most experiments and at most 10%.

A second possible experimental error is due to surface tension, resulting in a "small time gap between the start of the rainfall and the start of the surface runoff" (Cea et al, 2009). These effects are not considered in the numerical models and can lead to discrepancies between the numerical and experimental results. The effect becomes increasingly significant as rainfall intensity decreases. This is because surface tension effects are more important when the water depth is very shallow.

The third source of experimental error is due to a difference between the designed topography of the terrain as described above and the real topography used in the experiment. The designed topography of the domain is modelled as 3 planes each with a slope of 0.05. This topography is used in the numerical simulations. However, small deformations on the planes during setting up resulted in the real topography used in the experiments being substantially different from the designed topography. Figure 10 shows the difference between the designed and real topography as shown in Cea et al. (2009). It was noted in Cea et al. (2009) that it is important to define the topography of the domain in the numerical simulations accurately to obtain accurate results. "Using the designed topography produced much poorer results than using the real measured topography". The effect of real versus designed topography in numerical simulations will be shown when discussing the results of the simulations.

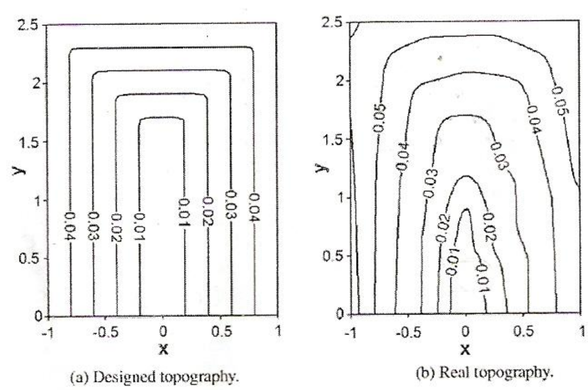

Figure 10(a,b)*: Ideal and Real Topography in Cea et al. (2009)*

3.4.2 Numerical model

A numerical mesh of 56481 elements and element size 1cm^2 was used in this simulation to represent the 2 x 2.5m domain as well as an additional 2 x 0.3m basin. The latter was added to generate rapid flows at the downstream boundary, so as to reproduce the effect of the sudden ground level decrease at the catchment outlet in physical experiments. The basin consisted of a continuous slope of 0.0005 from the end of the original domain. The grids range from 1 to 281 in the x-direction and 1 to 201 in the y-direction. Figure 11 shows an image of the topography used in the numerical simulations.

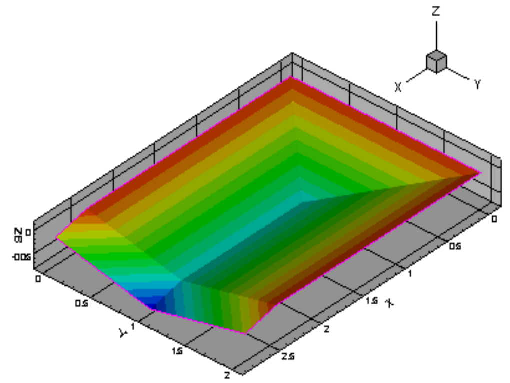

***Figure 11**: Computational Topography for the case in Cea et al. (2009)*

3 methods were used to represent the buildings in the domain, namely the Building-Hole, the Building-Block, and the Increased-Roughness method.

The Building-Hole (BH) method involves representing the buildings as holes in the numerical mesh such that any rainfall on the buildings are ignored. As the buildings occupy a significant proportion of the area in the domain, it is necessary to artificially increase the rainfall intensity to take into account the ignored rainfall. In the following simulations, the rainfall intensities used were obtained by dividing the input rainfall discharges by the net domain area that excluded areas occupied by the buildings. The buildings are however still represented as elevations in the topography and all water flows around the buildings.

The Building-Block (BB) method includes the buildings in the numerical mesh, with rainfall on the buildings being considered in the calculations. The buildings are incorporated into the mesh by increasing the bed elevation according to the heights of the buildings and an advantage is that it is physically more realistic as compared to the BH method. Movement of rainwater on the roof of buildings and the direction in which they fall onto the ground can be modelled. Also, it is not necessary to artificially increase the rainfall intensity (Cea et al, 2009). However, it is shown subsequently that numerical instabilities may occur and this will be discussed in later sections.

The Increased-Roughness (IR) method involves increasing the bed friction coefficient of areas occupied by buildings to a significantly larger value as compared to the surrounding surfaces. In the simulations carried out, the Manning's coefficient of the surfaces occupied by the buildings were increased from either n_m=0.01 or 0.016$m^{-1/3}s$ depending on the scenario to n_m=0.5$m^{-1/3}s$. The buildings are included in the numerical calculations but are no longer represented by elevations in the bed topography. Instead, all effects of the buildings are represented by the increased surface roughness. It is expected that the water velocities in the areas occupied by the buildings will be extremely low and water from surrounding areas will flow around the buildings as is the case in the experiments.

The only parameter that needs to be calibrated is the bed roughness coefficient which is represented by Manning's coefficient. Values of n_m=0.007, 0.01 and 0.016$m^{-1/3}s$ were used in various simulations and compared with experimental and numerical results from Cea et al. (2009). The minimum depth set to distinguish between a wet and dry element is 0.000001m and the time step used is either 0.005 or 0.01s depending on the simulation. The latter is checked to ensure that it satisfies the Courant condition.

Cea et al. (2009) modelled the topography and buildings using both the BH and BB method. Calibration of Manning's coefficient in Cea et al. (2009) was done using the Y20 layout and was set at n_m=0.016$m^{-1/3}s$. Although this is substantially higher than values of 0.010 and 0.012$m^{-1/3}s$ recommended in hydraulic manuals for smooth steel surfaces, this was found to be appropriate due to dust accumulation on the physical model and the extremely small water depths obtained which would lead to greater roughness. It was noted that the BH method was capable of representing the shape of buildings accurately with relatively coarse elements (Schubert et al, 2008). The BB method however required finer meshes around the buildings to represent their shape accurately and hence a BH method is more efficient in modelling flood inundation (Cea et al, 2009). Both methods were however capable of modelling "rapidly varying overland flow" with extremely shallow water depth, "highly unsteady wet-dry fronts, and high bed friction stresses" without "numerical instabilities and loss of precisions in the solution" (Cea et al, 2009). Also, the 2D models used in the numerical simulations cannot represent the movement of water from the roof to the ground accurately as the assumptions related to the shallow water model are broken locally. Hence velocities around the edge of the buildings cannot be assumed to be accurate (Cea et al, 2009). These factors should be considered when comparing the building representation methods subsequently.

3.4.3 Validation simulation results

Two building layouts based on Cea et al. (2009) were simulated and compared with experimental and numerical results by the above authors. Layouts X20 and Y20 were chosen as a complete set of experimental and numerical results by Cea et al. (2009) were available, and they provided simple configurations that allowed for a good understanding of some key features that may results from using the numerical model. The 25l/min Q25 hyetographs were chosen for the validation simulations as they provided the most extreme rainfall events with the highest rainfall intensity and hence prevented problems associated with surface tension and extremely shallow water depths. Overall, 25 simulations were carried out based on the 2 building layouts, 3 rainfall durations, 3 building representation methods and 3 surface roughness in different combinations. Figure 12(a,b) shows the building layouts X20 and Y20 respectively.

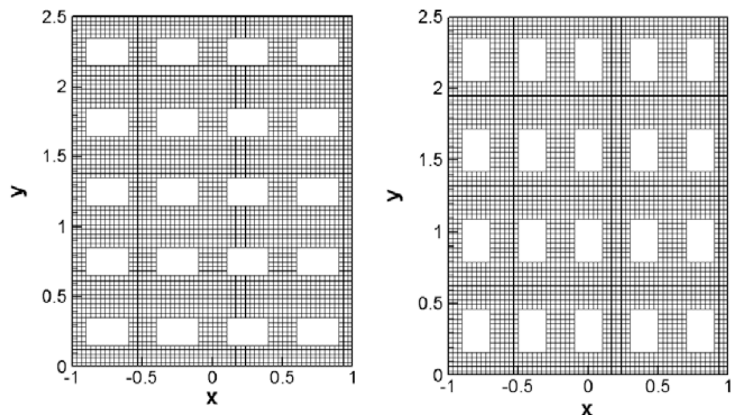

Figure 12(a,b)*: Building Layouts X20 and Y20 in Cea et al.(2009)*

3.4.3.1 Building layout X20

Building layout X20 consists of 20 buildings on the slopes straddling the central channel through which the water flow ultimately ends up. Figure 13(a,b) show the 3D model of the X20 layout used in the numerical analysis with the BH and BB methods from different view points.

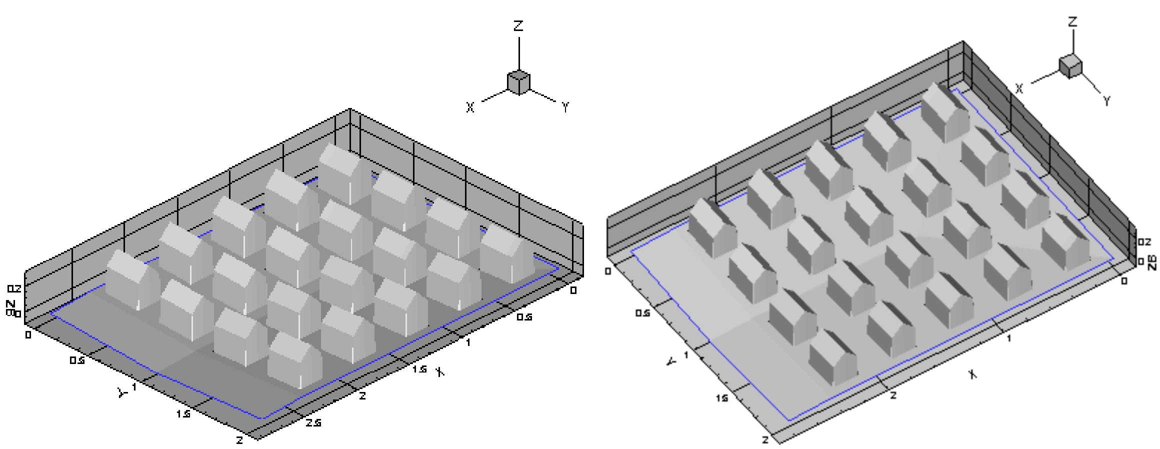

Figure 13(a,b)*: 3D model of Building Layout X20 from two different view points*

The rainfall-runoff simulation was conducted using the 3 aforementioned methods to represent the buildings and subjected to 3 rainfall hyetographs Q25T20, Q25T40 and Q25T60. 2 values of Manning's coefficient, n_m=0.01 and 0.016$m^{-1/3}s$ were used to determine which matched the experimental results better. An additional simulation using the BH method with n_m=0.007$m^{-1/3}s$ was carried out with Q25T60 to determine the effect of changing Manning's coefficient. The results of discharge Q_x (m^3/s) against time t (s) for the 3 hyetographs are shown in Figure 14, 15 and 16. In addition, the experimental and numerical results by Cea et al. (2009) are also plotted.

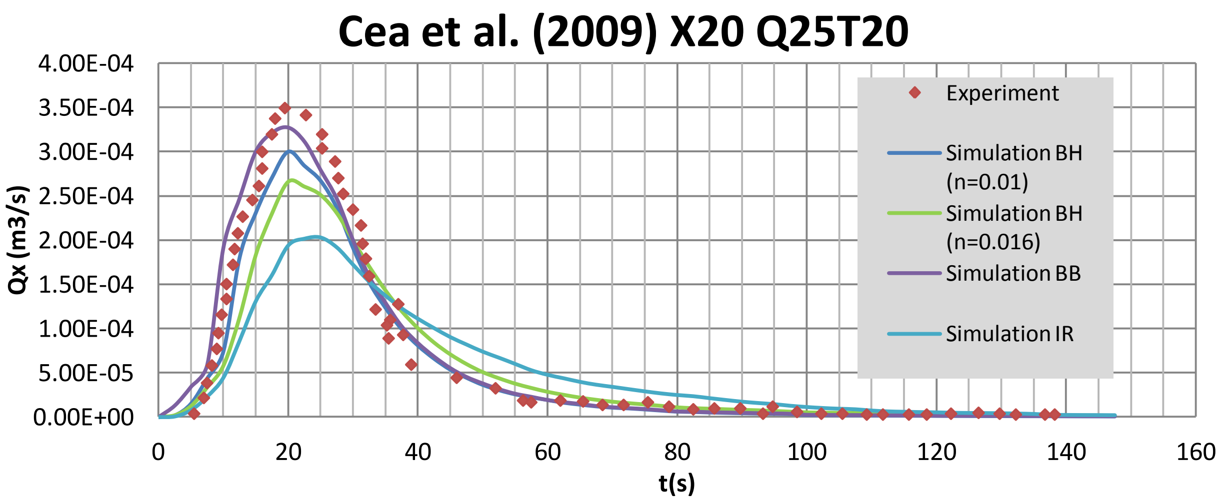

***Figure 14**: Validation Results for X20 and Q25T20*

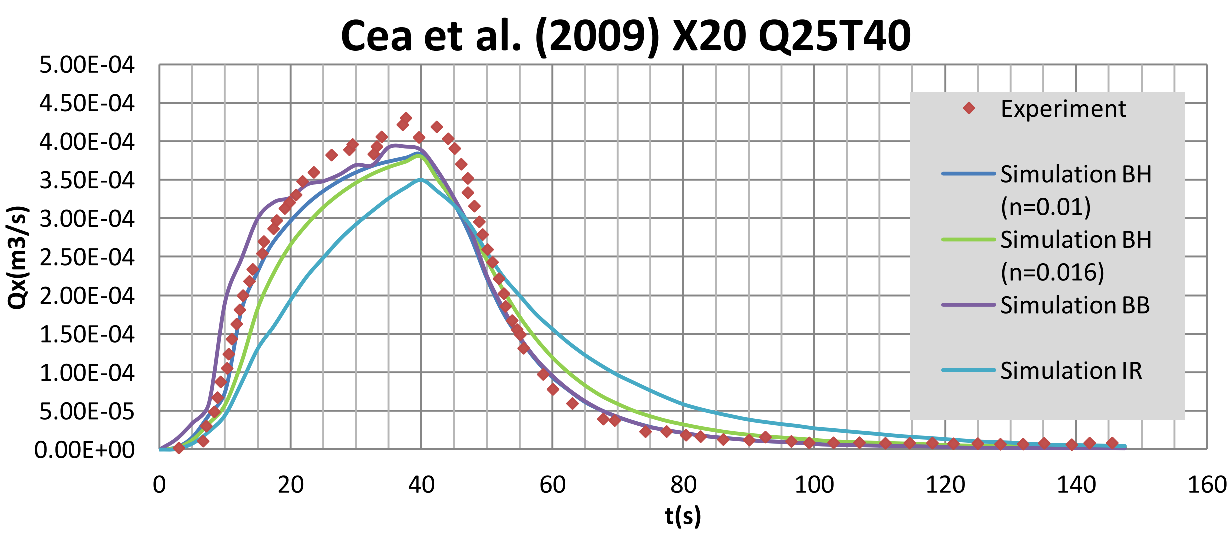

***Figure 15**: Validation Results for X20 and Q25T40*

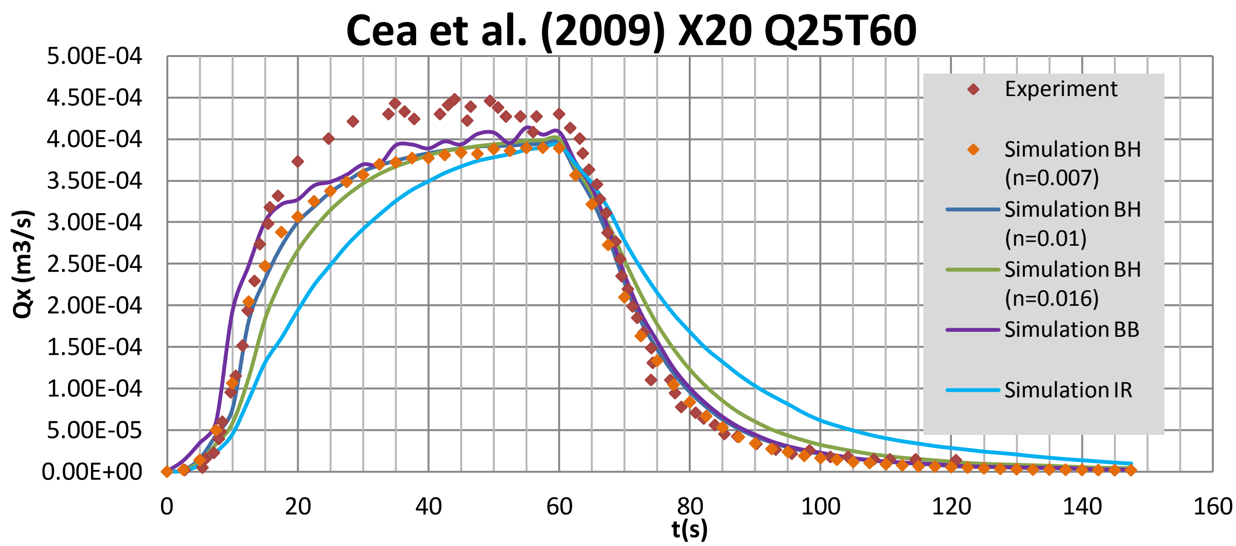

***Figure 16**: Validation Results for X20 and Q25T60*

3.4.3.2 Building layout Y20

Similarly to X20, layout Y20 consists of 20 buildings lying on the slopes of the terrain. However, the orientations of the buildings have changed and 4 buildings now straddle the central channel of the domain. Simulating this layout would provide an insight into the possible effects that may result when the numerical model simulate flows that are blocked by buildings. Figure 17(a,b) show the 3D model of the Y20 layout used in the numerical analysis with the BH and BB methods from two different view points.

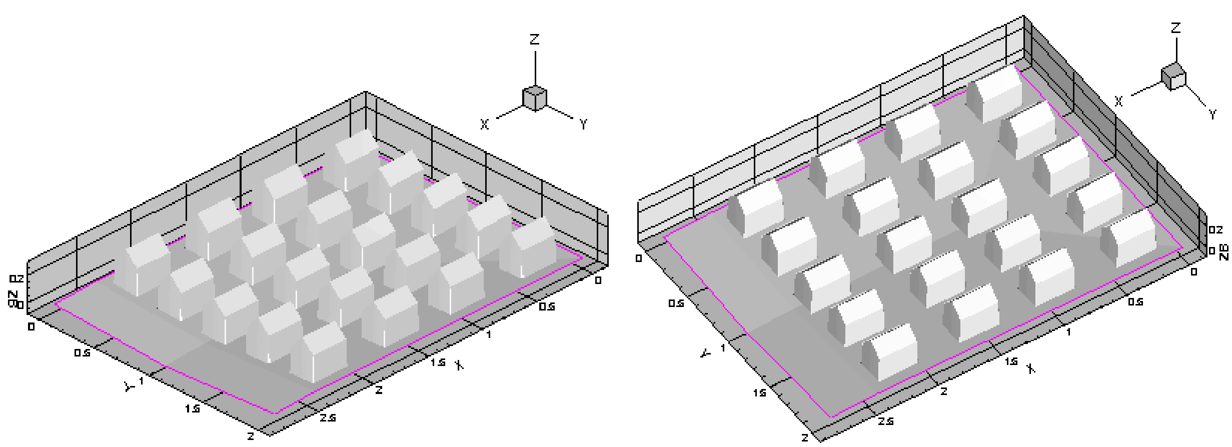

***Figure 17(a,b)**: 3D Model of Building Layout Y20 from two different view points*

Rainfall-runoff simulations were conducted using the BH, BB and IR methods to represent the buildings. The domain was once again subjected to 3 rainfall hyetographs Q25T20, Q25T40 and Q25T60. Manning's coefficient n_m=0.016$m^{-1/3}$s was used as stated in Cea et al. (2009). 3 additional simulations were carried out using n_m=0.01$m^{-1/3}$s and the BH method to observe the effects of changing the bed roughness for the Y20 configuration. Overall, 12 validation simulations were carried out.

In addition to the experimental results, Cea et al. (2009) provided simulation results using the designed topography to which this project's simulation results can be compared to. This was available for the Y20 Q25T20 and Y20 Q25T40 scenarios. Figure 18, 19 and 20 show the results obtained from the simulations as well as the experimental and simulation results obtained from Cea et al. (2009).

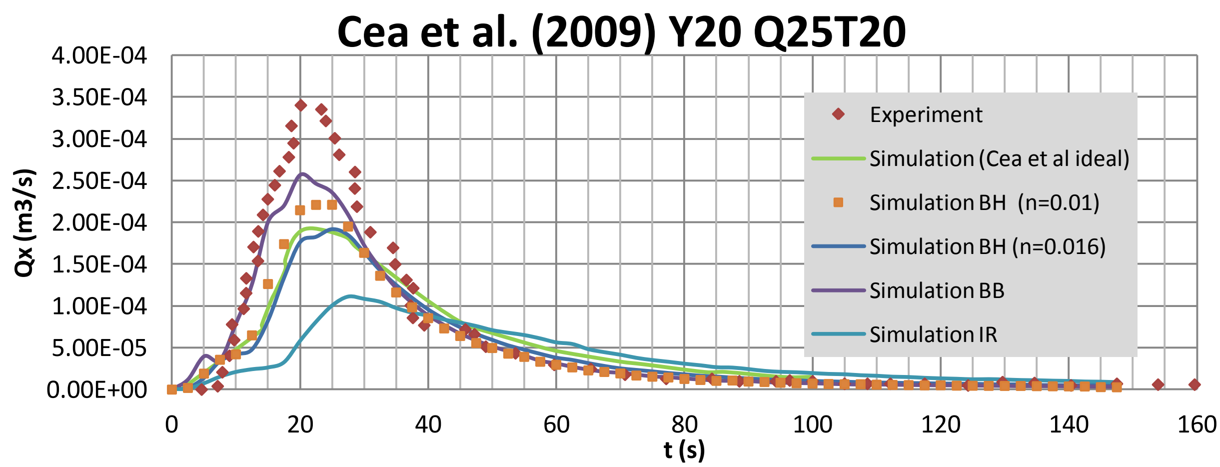

Figure 18*: Validation Results for Y20 and Q25T20*

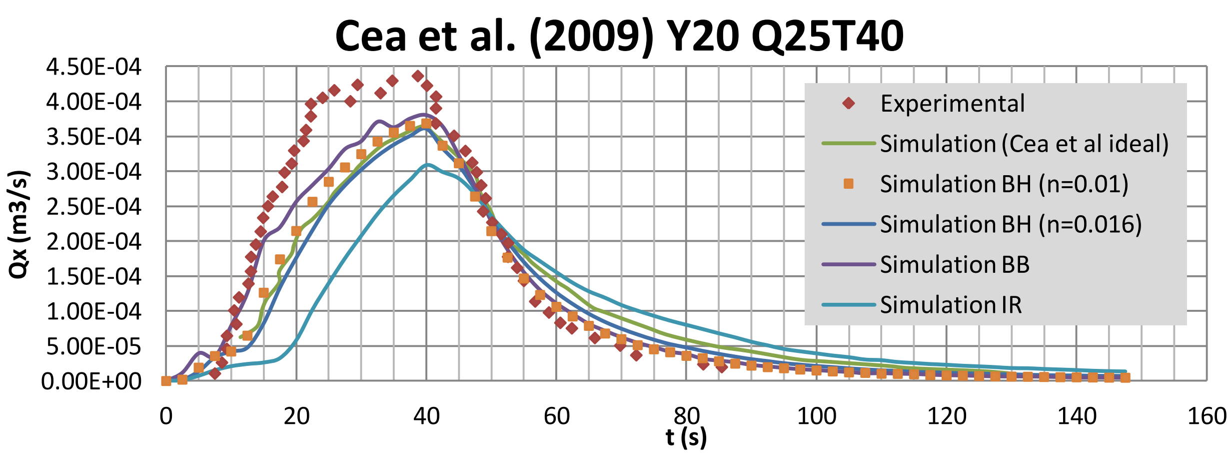

Figure 19*: Validation Results for Y20 and Q25T40*

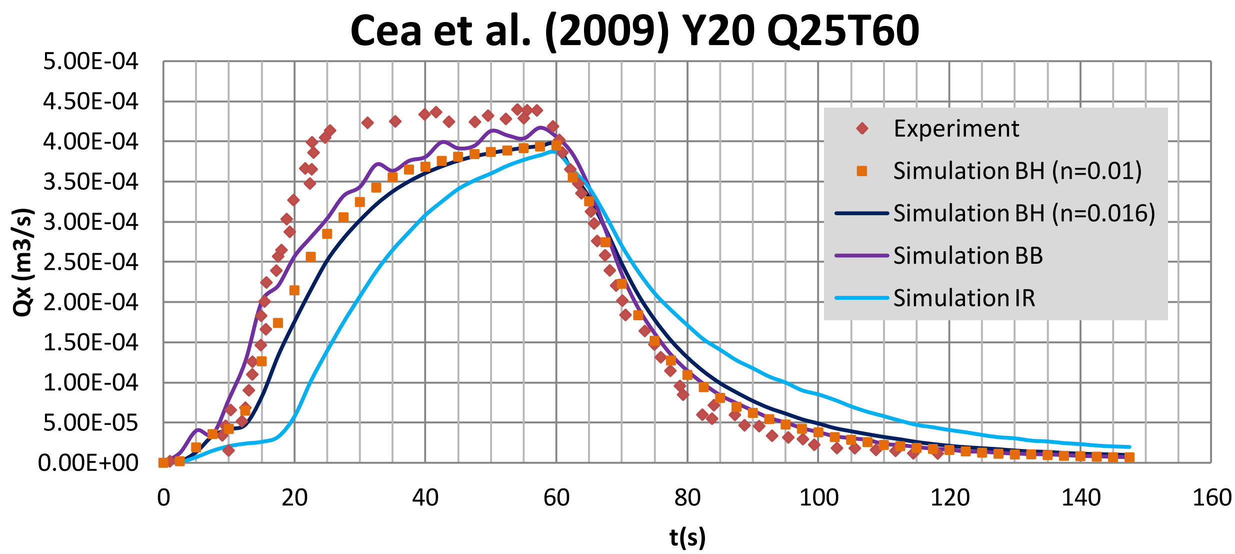

Figure 20: *Validation Results for Y20 and Q25T60*

3.4.4 Comparison between the three building representation methods

This section will focus on the comparison of the Building-Hole (BH), the Building-Block (BB), and the Increased-Roughness (IR) methods in representing the buildings.

3.4.4.1 Peak discharges

Results from simulations involving layouts X20 and Y20 have shown that in general, the BB method produced the largest peak discharge followed by the BH and subsequently the IR method. A summary of the peak discharges obtained from the 3 methods, the experiment and simulations carried out by Cea et al. (2009) is shown in Table 3.

Table 3: *Summary of peak discharges for layouts X20 and Y20, Q25T20, Q25T40, Q25T60*

	X20 (x10^{-4} m^3/s)			**Y20 (x10^{-4} m^3/s)**		
	20s	**40s**	**60s**	**20s**	**40s**	**60s**
Experiment	3.5	4.22	4.3	3.40	4.36	4.39
Cea et al. Ideal				1.91	3.61	
BH (n=0.007m$^{-1/3}$s)			3.89			
BH (n=0.01m$^{-1/3}$s)	3.0	3.83	3.89	2.21	3.61	3.95
BH (n=0.016m$^{-1/3}$s)	2.66	3.8	3.89	1.91	3.61	3.96
BB	3.27	3.93	4.09	2.57	3.81	4.17
IR	2.01	3.49	3.9	1.11	3.08	3.83

3.4.4.2 Effects of designed versus real topography

All simulations carried out produced discharges that were smaller than the experimental results. This is due to differences between the designed and real topography as described in section 3.4.1. Numerical simulations carried out by Cea et al. (2009) using the Y20 configuration, ideal topography and n_m=0.016$m^{-1/3}$s for Q25T20 and Q25T40 produced results that are similar to that carried out using n_m=0.016$m^{-1/3}$s in this project. This shows the importance of using an accurate representation of the topography in the simulations.

3.4.4.3 Discrepancies in peak discharge and volume of discharge

In general, the BB method appears to produce a higher volume of discharge. This is indicated by the larger area under the discharge Q_x (m^3/s) versus time t(s) graphs shown in Figures 14 to 16 and 18 to 20. The apparent differences in total discharge when using the different methods are due to the differences in volume of water remaining in the domain at the end of the simulation. Considering the Y20 Q25T20 simulation at t=150s, the volume of water remaining in the BH and BB domain are 1.285x10^{-3} m^3 and 3.304x10^{-4} m^3 respectively, giving a difference in volume of 9.546x10^{-4} m^3. From the graphs, the difference in total discharge volume between the BB and BH method is approximately 1.0x$10^{-3}$$m^3$ which is similar to the difference between the final domain volumes shown above. Hence, the total volume of water when using the 2 methods are similar, with a lower discharge using the BH method resulting in a larger volume of water remaining in the domain at the end of the simulation. Table 4 shows a summary of the above results for both layouts X20 and Y20.

***Table 4**: Differences in discharge volumes from the BH and BB methods, X20 and Y20, Q25T20*

	X20 (m^3)	**Y20 (m^3)**
Volume of water remaining in the domain at t=150s using the BH method $V_{BH, 150s}$	3.507x10^{-4}	1.285x10^{-3}
Volume of water remaining in the domain at t=150s using the BB method $V_{BB,150s}$	-6.106x10^{-4}	3.304x10^{-4}
$V_{BH,150s} – V_{BB,150s}$	9.613x10^{-4}	9.546x10^{-4}
Difference in water volume within the domain between the BB and BH graphs (approximate)	1.0x10^{-3}	1.0x10^{-3}

3.4.4.4 Differences in rate of increase of discharge between BB and BH method

The larger discharge produced initially when using the BB method is likely due to the way in which the numerical model is set up. With the BB method, the rainfall intensity is constant everywhere in the domain. With the BH method however, the rainfall intensity is zero above the buildings and artificially increased elsewhere in the domain to maintain a constant input of water. Hence, it takes a longer time for the same volume of water to reach the outlet of the domain with the BH method as compared to the BB method, resulting in the larger discharge with the BB method initially.

3.4.4.5 Instabilities associated with the BB method

The fifth feature observed is the instabilities in the numerical simulation that occur when using the BB method and these are particularly significant in the T60 cases as shown in Figures 16 and 20. The large bed elevation gradients at the edges of buildings result in particularly high water velocities. To ensure mass conservation, the depth at certain points may become negative and although the simulation remains stable globally, local instabilities in the numerical calculations may occur. The negative volume remaining in the domain at the end of the simulation for layout X20 subjected to Q25T20 hyetograph when using the BB method is due to the same reason of mass conservation.

In the numerical model, the change in volume of water in an element is equal to the net volume of water entering or leaving the cell.

$$A\frac{\Delta D}{\Delta t} = \sum Q \tag{5}$$

where A is the area of an element, ΔD is the change in depth in the element, Δt is the time step and $\sum Q$ is the net discharge into a cell.

From equation (5),
$$A\frac{\eta_{t+\Delta t}-\eta_t}{\Delta t} = \sum Q$$

$$\eta_{t+\Delta t} = \frac{\sum Q\ \Delta t}{A} + \eta_t \tag{6}$$

where η_t and $\eta_{t+\Delta t}$ are the water level at time t and $t+\Delta t$ respectively.

When the velocity of water at the edge of the building is too high, the net discharge $\sum Q$ of the element at the edge of the building is negative to take into account the volume of water leaving that particular cell. If η_t is smaller than the $\frac{\sum Q\,\Delta t}{A}$ term, the water level $\eta_{t+\Delta t}$ will become negative. The model does not take into account the bed elevation of the cell and hence the water level is allowed to become smaller than the bed elevation, resulting in negative water depth. To prevent the occurrence of negative depth, it is possible to reduce the time step Δt of the simulation while still ensuring that it fulfils the Courant condition. As an example, Figure 21(a,b) shows the water depth in the domain at t=40s when layout X20 is subjected to Q25T60 hyetograph and simulation is carried out using the BB and BH method with n_m=0.01m$^{-1/3}$s respectively. Negative water depth is observed around the edges of the buildings when the BB method is used.

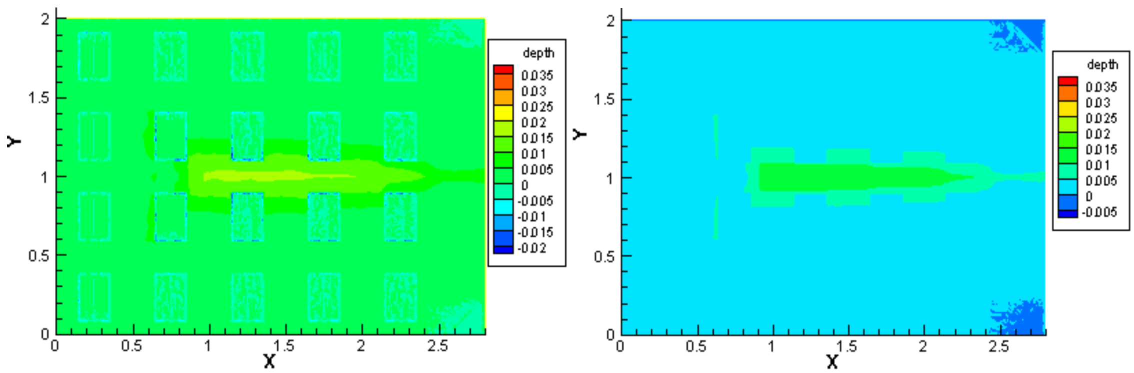

Figure 21(a,b)*: Water depth profile for X20 and Q25T60 using BB and BH methods*

3.4.4.6 Increase-Roughness method

A third method of representing the buildings is the Increased-Roughness (IR) method. The entire topography of the domain is flat and the areas occupied by the buildings have increased bed surface roughness of Manning's coefficient n_m=0.5m$^{-1/3}$s. Essentially, the water velocities on the areas occupied by the buildings are close to zero due to the high surface roughness. Water depth on these areas thus increases over time and water from other parts of the domain flow around the "buildings" as would be the case physically. The change in water depth over the "buildings" over time and the flow of water around the "buildings" for the Y20 layout subjected to Q25T20 hyetograph can be seen in Figure 22.

This method has however produced peak discharges that are much smaller than the experimental results and that using other methods. Also, the increase and decrease in discharge occurs much more slowly. These effects are attributed to the collection of water over the "buildings" that do not contribute to the discharge in the initial stages of the simulation but are slowly released later on when surrounding water velocity and depth decreases. Hence, this method of representing the buildings is the least effective among the 3 suggested methods.

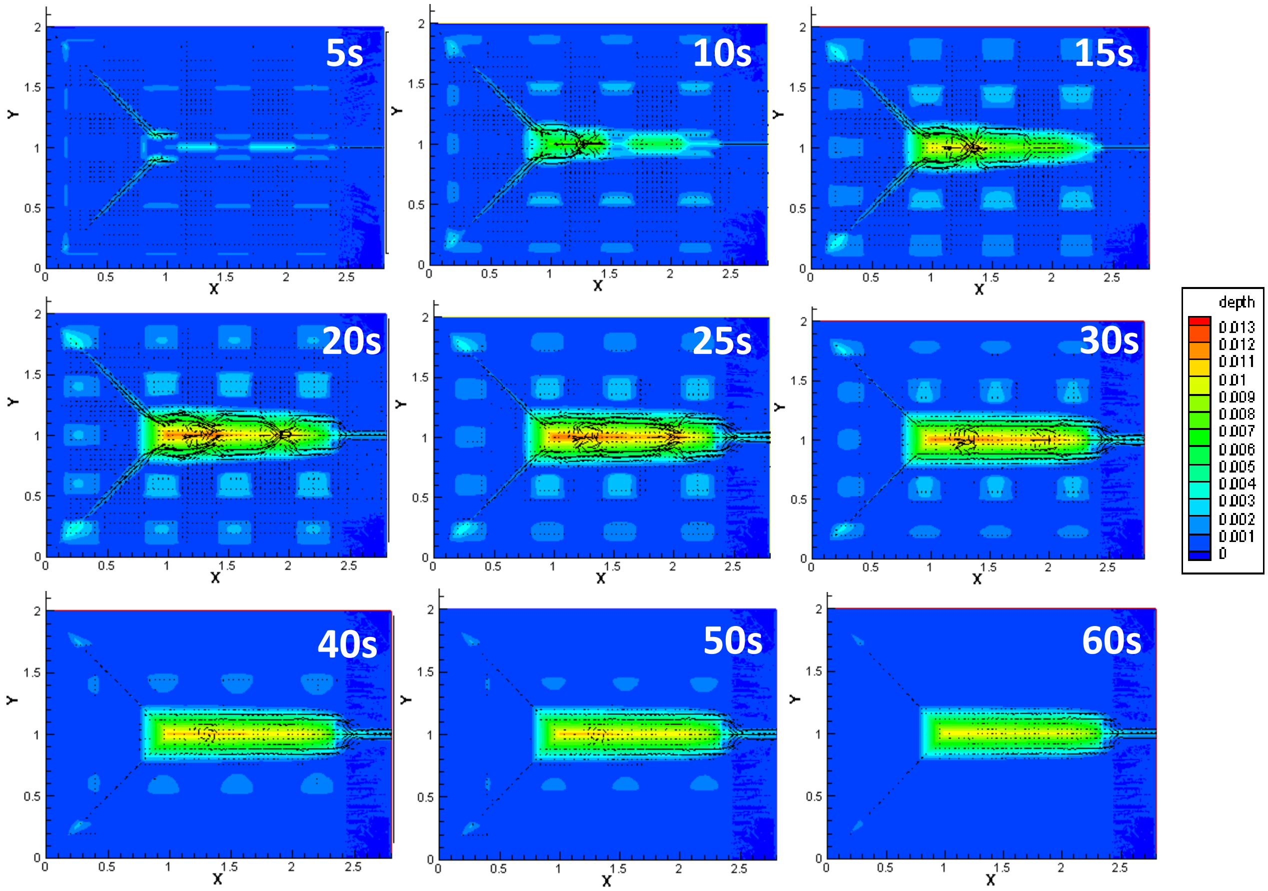

Figure 22:*Development of water depth distributions for Y20 layout using IR method*

<u>3.4.4.7 Effect of layout on building representation method</u>

Simulations using layouts X20 and Y20 have produced different results. Firstly, the BB method produced results that better match the experimental results for layout Y20 as compared to the BH method. However, the opposite is true for layout X20. This is observed from the hydrographs in Figures 14 to 16 and 18 to 20. Secondly, the differences between the experiment and simulation results are more significant for Y20 as compared to X20. Table 5 shows the differences between the peak discharges obtained using the 3 methods and the experiment for layouts X20 and Y20 under 25 l/min discharge. These 2 differences are likely due to the increase importance of the difference between the designed and real topography when simulating the Y20 layout and is attributed to the way in which the buildings are arranged in the domain. In layout Y20, 4 buildings span the central channel of the domain through which water flows out of the domain. The central channel in the X20 configuration is however clear with all buildings lying on the adjacent slopes. Hence, water can flow out of the X20 domain much more easily and is less likely to become trap in the channel as compared to layout Y20. Features such as this should be considered in future simulations as possible sources of error.

***Table 5**: Difference in peak discharges for layouts X20 and Y20, Q25T20, Q25T40, Q25T60*

Building Representation Method	**Q25T20**		**Q25T40**		**Q25T60**	
	X20 (m^3/s)	**Y20 (m^3/s)**	**X20 (m^3/s)**	**Y20 (m^3/s)**	**X20 (m^3/s)**	**Y20 (m^3/s)**
Building Hole (n_m=0.016$m^{-1/3}$s)	8.4×10^{-5}	1.49×10^{-4}	4.2×10^{-5}	7.5×10^{-5}	4.1×10^{-5}	4.3×10^{-5}
Building Block	2.3×10^{-5}	8.3×10^{-5}	2.9×10^{-5}	5.5×10^{-5}	2.1×10^{-5}	2.2×10^{-5}
Increased Roughness	1.49×10^{-4}	2.29×10^{-4}	7.3×10^{-5}	1.28×10^{-4}	4.0×10^{-5}	5.6×10^{-5}

3.4.4.8 Effect of rainfall duration

Generally, the effects of differences between the real and designed topography and changes in the Manning's coefficient on the building representation methods are most significant when the duration of the rainfall is the shortest. Referring to Table 5, the difference between the peak discharges obtained in the Y20 experiment and from simulations using the BB method is 8.3 x $10^{-5}m^3/s$ for the T20 case, $5.5 \times 10^{-5}m^3/s$ for the T40 case and $2.2 \times 10^{-5}m^3/s$ for the T60 case. The differences in peak discharges from using n_m=0.01$m^{-1/3}$s and n_m=0.016$m^{-1/3}$s are $3 \times 10^{-5}m^3/s$ and $1 \times 10^{-5}m^3/s$ for the T20 and T40 cases respectively and negligible for the T60 Y20 case. Also, the differences between the experiment results and simulations using the ideal topography are $1.49 \times 10^{-4}m^3/s$ and $7.5 \times 10^{-5}m^3/s$ for the T20 and T40 case respectively. These are probably due to the shallower water depth and hence greater surface tension associated with shorter rainfall duration and discharge.

Overall, features that need to be considered when using the numerical model for future simulations are the need to define the topography accurately and how the arrangement of buildings may affect the discharge if they interfere with the flow path significantly. 3 methods of representing buildings were considered and the BH method has been selected for future simulations. Inaccuracies in the results obtain with the IR method and instabilities associated with using the BB method have made the BH method the most desirable. Generally, changing the Manning's coefficient has not affected the discharge significantly especially for higher rainfall durations and steel surfaces will be represented by n_m=0.01$m^{-1/3}$s in future simulations.

4. Model Application-Parametric Study

The second stage of the project after validating the numerical model against published analytical and experimental results is the parametric study. The numerical model is used to investigate the effects of various factors on the surface runoff in an urban setting which will be useful for urban drainage design and risk management. Factors that will be investigated in this project include the layout of the buildings on the slope, the density of the buildings and the effect of different terrain slopes. The building layouts used are the Y20, Y12, X20, X12, S20 and S12 layouts used in Cea et al. (2009). Four plane slopes of 0.5%, 1%, 3% and 5% are considered. Lastly, the rainfall intensities imposed on the domain are based on discharges of 7, 15 and 25 l/min and duration of 10, 20, 40 and 60s. A total of 78 simulations were carried out to investigate the effects of the various factors on the surface runoff. The different factors, simulation results and possible sources of error will be discussed.

4.1 Scope of the study

Factors that are investigated are the building layout, the building density and the slope.

6 building layouts were investigated in this study based on layouts Y20, Y12, X20, X12, S20 and S12 proposed in Cea et al. (2009) and shown in Figure 9. These 6 layouts represent 3 different ways in which the buildings are arranged and 2 building densities. The Y and X layouts have all the buildings with their lengths parallel and perpendicular to the direction of water flow down the slope respectively. Alternatively, the S layout is a combination of both the Y and X layouts with buildings in a staggered arrangement.

In addition, the 20 and 12 extensions represent 2 building densities, with 20 buildings in each of the first domain and 12 in the latter. Although these 6 layouts are simplified representations of actual urban layouts, they provide a good starting point for studies of urban surface runoff and give an opportunity for identifying potential sources of error or problems in using the numerical model. Figure 23 and Figure 24 show the numerical mesh and 3D images of the 6 layouts used in this study.

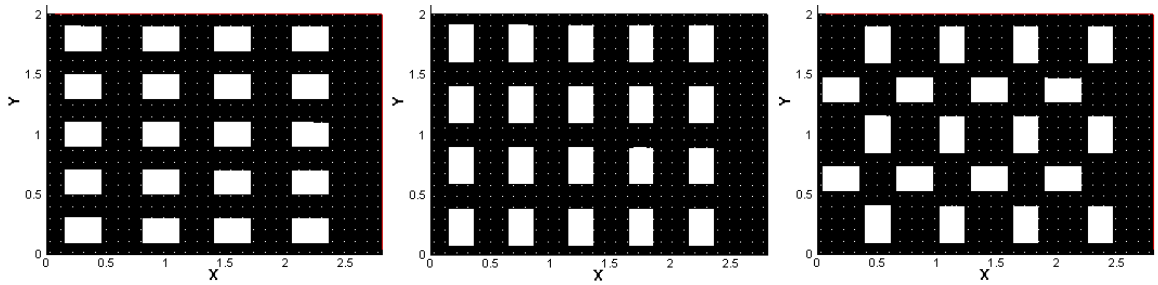

Figure 23(a,b,c)*: Layouts Y20, X20, S20*

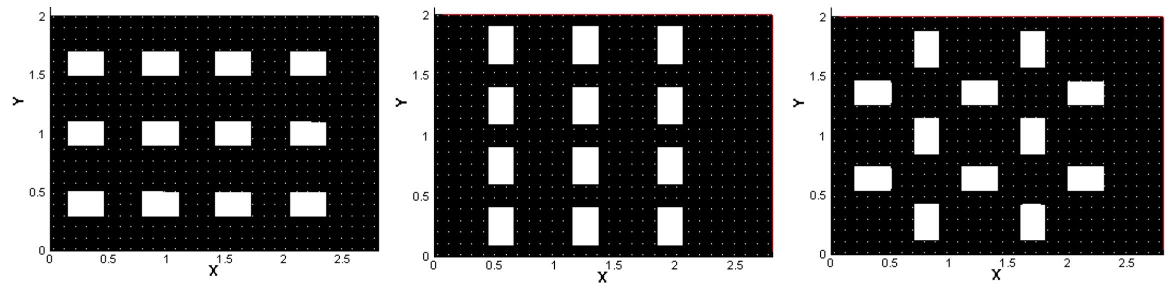

Figure 23(d,e,f)*: Layouts Y12, X12, S12*

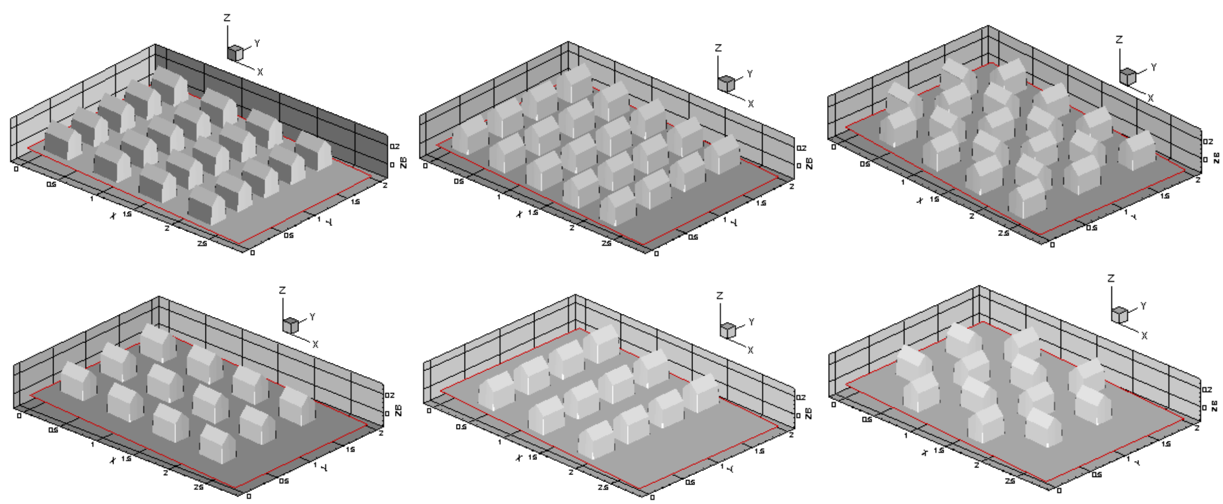

Figure 24(top: a,b,c; bottom: d,e,f)*: 3D visualisation of Y20, X20, S20, Y12, X12, S12 layouts*

The third factor considered is the slope of the terrain. 4 slopes of 0.5%, 1%, 3% and 5% are considered to represent a general range of slopes from flat to steep in an urban setting. Each of the 6 layouts will be subjected to the Q25T10 rainfall to investigate the effects of slope on each of the layout. The discharge was chosen as it represented the most extreme discharge and the short duration prevented steady state from occurring. In addition, the Y20 layout was subjected to Q25T20 and Q25T40 rainfall as a representative scenario to investigate the effects of the changes in rainfall duration on the influences caused by the slope.

The rainfall hyetographs imposed in the simulations are based largely on Cea et al. (2009) as shown in Table 2. As the terrains in the parametric studies are single plane slopes, the time of concentration are expected to be faster than those in the validation tests. An additional rainfall duration of 10s is hence included to investigate scenarios in which steady state flow is not achieved.

4.2 Numerical model

Similar to the validation tests, a numerical mesh of 56481 elements of element size $1cm^2$ was used to represent the 2 x 2.5m domain and 2 x 0.3m basin into which water can flow into to avoid collecting in the main domain. The grids range from 1 to 281 in the x-direction and 1 to 201 in the y-direction. To simplify the development of the numerical input model as compared to that used in the validation tests, a continuous slope is present throughout the entire domain including the end basin. The default slope of the terrain is set at 5% unless otherwise stated. 3D images of the simulation domains are shown in Figure 24.

The Building-Hole (BH) method was chosen to represent the buildings or obstructions following the validation tests as the method provided the best balance of stability and accuracy in the numerical simulation. As the buildings occupy a significant proportion of the domain and rainfall on the buildings are not included in the calculations, it is necessary to artificially increase the intensity of the input rainfall. This is achieved by dividing the total discharge over the net area of the domain that excludes the areas occupied by the buildings and basin. Rainfall is only set to fall between grids 1 to 251 in the x-direction and the output hydrograph is obtained by measuring the discharge along the X=251 plane. Details of the BH method can be found in section 3.4.2: Numerical simulations.

In all of the following simulations, the Manning's coefficient is calibrated as $0.01m^{-1/3}s$. A nominal value of 0.000001m is set as the minimum depth as before, and a time step of Δt=0.01s and grid size Δx=0.01m are used.

4.3 Comparison between building layouts

4.3.1 Simulations

The 6 building layouts Y20, Y12, X20, X12, S20 and S12 are subjected to 3 rainfall discharges of 10s duration to investigate their influence on the surface runoff. The 3 input hyetographs of Q7T10, Q15T10 and Q25T10 represent input rainfall discharges of 7, 15 and 25 l/min respectively. The range of discharges enables the significance of the layouts when subjected to different rainfall intensities to be studied. In addition, instabilities or problems relating to the simulations may be observed by comparing results across the different discharges. This is especially plausible when low discharges such as 7 l/min are involved.

In addition, the 6 layouts were subjected to the Q25T40 hyetographs with terrain slopes of 5% and 3% and Q25T60 hyetograph with terrain slope of 1% to observe the effects on the time of concentration of the runoffs.

A total of 36 simulations were carried out to investigate the influence of building layout on the surface runoff.

4.3.2 Output hydrographs

Figure 25 to 30 show the hydrographs obtained from the 6 layouts when subjected to the Q7T10, Q15T10, Q25T10, Q25T40 for slopes of 5% and 3%, and Q25T60 hyetograph for slopes of 1%.

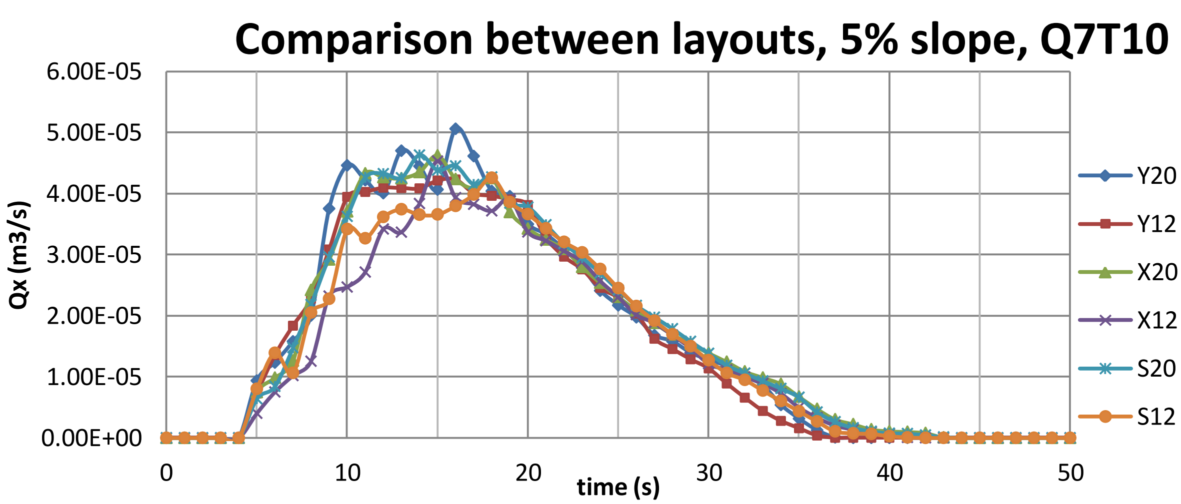

***Figure 25**: Comparison between layouts with 5% slope and Q7T10*

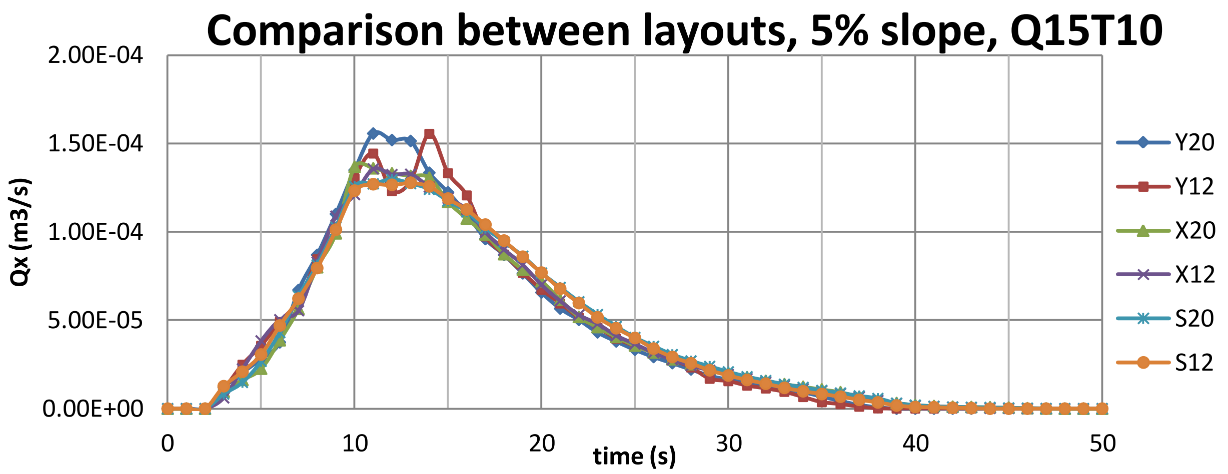

Figure 26*: Comparison between layouts with 5% slope and Q15T10*

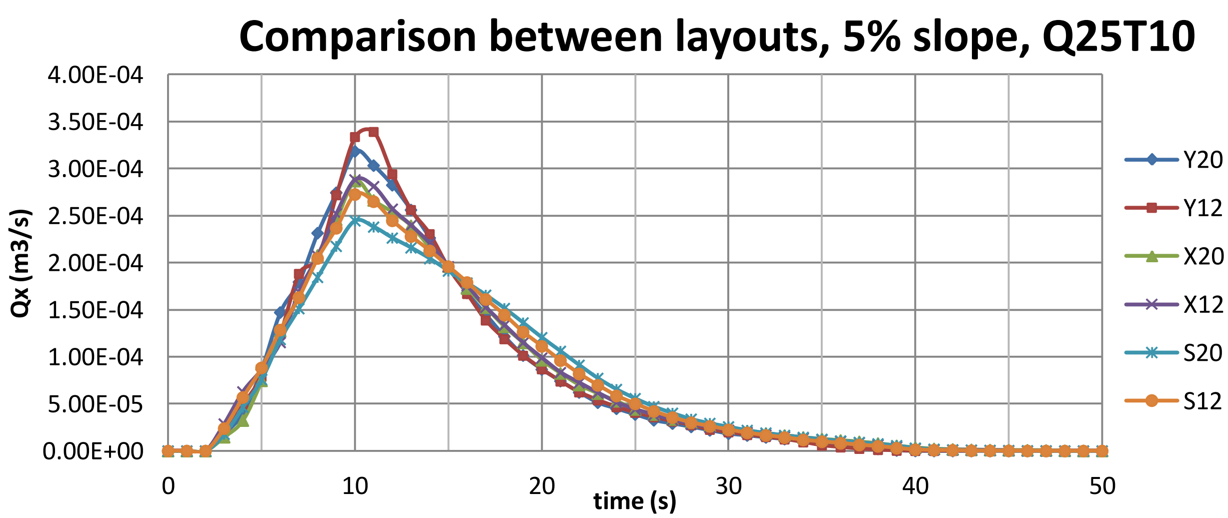

Figure 27*: Comparison between layouts with 5% slope and Q25T10*

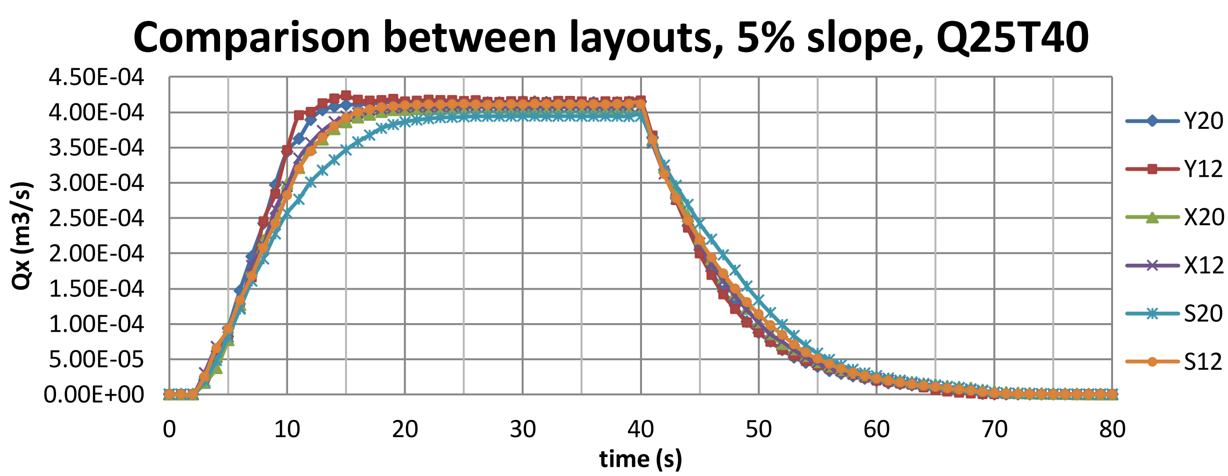

Figure 28*: Comparison between layouts with 5% slope and Q25T40*

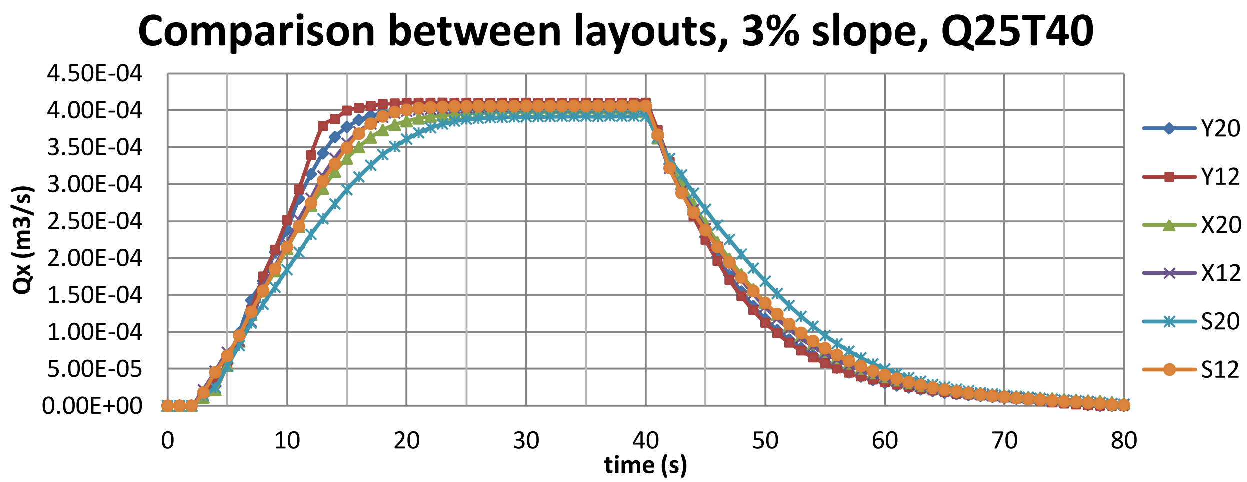

Figure 29*: Comparison between layouts with 3% slope and Q25T40*

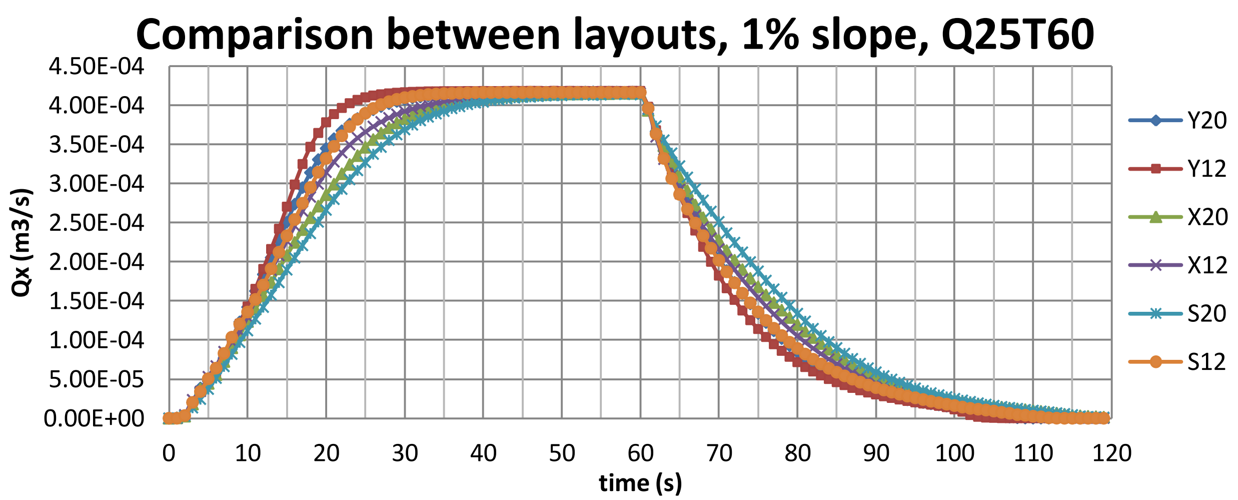

Figure 30*: Comparison between layouts with 1% slope and Q25T60*

4.3.3 Discussion

4.3.3.1 Q25T10, Q25T40 with 5% and 3% slope, Q25T60 with 1% slope

It is expected that the Y layouts will produce the largest discharge followed by the X and lastly the S layouts. The time of peak discharge or concentration also increases from Y to X and S layouts. This is seen in Figure 27 to 30 in which the domain is subjected to 25 l/min of rainfall for 10, 40 or 60s. In Figure 27 for example, the Y12 layout produces the largest discharge of 0.000339m^3/s followed by X12 with 0.000288m^3/s and S12 with 0.000273m^3/s. A similar relationship is seen with Y20, X20 and S20 in Figure 27. Table 6 shows a summary of the time of peak discharge or concentration and peak discharge for each of the layouts when subjected to 25 l/min of rainfall for 10s and 40s with 5% slope, and 60s with 1% slope.

***Table 6**: Summary of time of concentration and peak discharges for the 6 layouts*

Layout	Q25T10, 5% slope		Q25T40, 5% slope		Q25T60, 1% slope	
	Time of peak discharge t_p (s)	**Peak discharge (m^3/s)**	**Time of concentration t_c (s)**	**Peak discharge (m^3/s)**	**Time of concentration t_c (s)**	**Peak discharge (m^3/s)**
Y20	10.0	3.18×10^{-4}	17.0	4.14×10^{-4}	47.0	4.17×10^{-4}
X20	10.0	2.87×10^{-4}	23.0	4.05×10^{-4}	52.0	4.15×10^{-4}
S20	10.0	2.45×10^{-4}	25.0	3.94×10^{-4}	52.0	4.14×10^{-4}
Y12	11.0	3.39×10^{-4}	14.0	4.17×10^{-4}	32.0	4.18×10^{-4}
X12	10.0	2.88×10^{-4}	20.0	4.07×10^{-4}	48.0	4.15×10^{-4}
S12	10.0	2.73×10^{-4}	21.0	4.11×10^{-4}	37.0	4.15×10^{-4}

4.3.3.2 Q7T10

The relationship between the Y, X and S layouts as observed in Figures 27 to 30 with 25 l/min discharge is not observed in Figure 25 with input discharge of 7 l/min. In general the differences between the hydrographs obtained with the lower input discharge were less significant and layout Y20 produced a hydrograph with 3 peaks. Instabilities in the discharge are also observed with layouts X20, X12, S20 and S12. These instabilities and multiple peaks could be due to vortexes in the flow causing backflow at the output plane. As the discharges observed in Figure 25 are very small and on the order of $0.000001 m^3/s$, small backflows will be significant and easily observed as compared to the cases with higher input discharges. Furthermore, the small water depths could mean that the effects of surface tension are greater and could result in inaccurate results.

4.3.3.3 Q15T10

The relationship between the layouts seen in Figure 26 when the domains are imposed with 15 l/min of rainfall is also less significant compared to cases with 25 l/min of discharge. The X and S layouts produced relatively similar peak discharges. However, peak discharges produced with the Y layouts were significantly larger. For example, all the X and S layouts produced peak discharges in the region of 1.3x10^{-4}m^{3}/s. The Y layouts however produced peak discharges in the region of 1.5x10^{-4}m^{3}/s.

In addition, layout Y12 produced a hydrograph with 2 peaks. As mentioned above, the 2 peaks could be due to vortexes that form near the output plane, causing backflow.

4.3.3.4 Discrepancy in peak discharges

Although the pattern of shorter time of concentration for the Y followed by X and S layouts is expected, the significantly larger peak discharge for the Y12 layout and lower peak discharge for the S20 layout as seen in Figure 28 are unexpected and could represent computation errors associated with the numerical simulations. Layout Y12 produced a peak discharge of 4.17x10^{-4} m^{3}/s while S20 produced a peak discharge of 3.94x10^{-4}m^{3}/s. No significant changes in the water depths are observed during steady state and hence this problem cannot be attributed to a build-up of water in the domain over time.

Further simulations involving 25 l/min of rainfall on smaller slopes of 3% and 1% were carried out to investigate if numerical errors could have occurred when the slope is large and the flow is rapid. The results from the new simulations are shown in Figures 29 and 30. The range of peak discharges appear to decrease from 2x10^{-5}m^{3}/s with 5% slope to 1.84x10^{-5}m^{3}/s with 3% slope and 3x10^{-6}m^{3}/s with 1% slope. Hence, it is expected that the discrepancy is due to numerical errors associated with rapid flows and these should be considered in future simulations.

Overall, the numerical simulations carried out have shown that the layout of buildings have an effect on the surface runoff. In general, the discharges are largest when buildings are aligned with their length parallel to the direction of the water flow. This is expected as there are fewer obstructions that block the path of water down the slope. On the other hand, the S layouts with their staggered arrangement of buildings provide greater obstruction and reduce the rate of discharge out of the domain. Build-up of water could hence occur in the domain and represent flooding in urban areas in real scenarios. Although modifications must be made to the numerical model to ensure stability in scenarios involving steep slopes or small discharges, these simulations show the applicability of the numerical model in studying the effects of building layout on urban surface runoff.

4.4 Comparison between slopes

4.4.1 Simulations

Each of the 6 layouts were imposed on 4 slopes of 0.5%, 1%, 3% and 5% and subjected to rainfall of 25 l/min and 10s duration. In addition, layout Y20 was subjected to the Q25T20 and Q25T40 hyetographs to observe if the volume of input rainfall affects the influence of the slopes significantly. The slopes were chosen to represent a range of terrain from flat to steep. Overall, 32 simulations were carried out to investigate the effect of terrain slope on the surface runoff.

4.4.2 Output hydrographs

Figure 31(a-f) shows the hydrographs obtained from layouts Y20, Y12, X20, X12, S20 and S12 when subjected to the Q25T10 hyetograph respectively. In addition, Figures 32 and 33 show the hydrographs obtained when layout Y20 is subjected to the Q25T20 and Q25T40 hyetographs respectively.

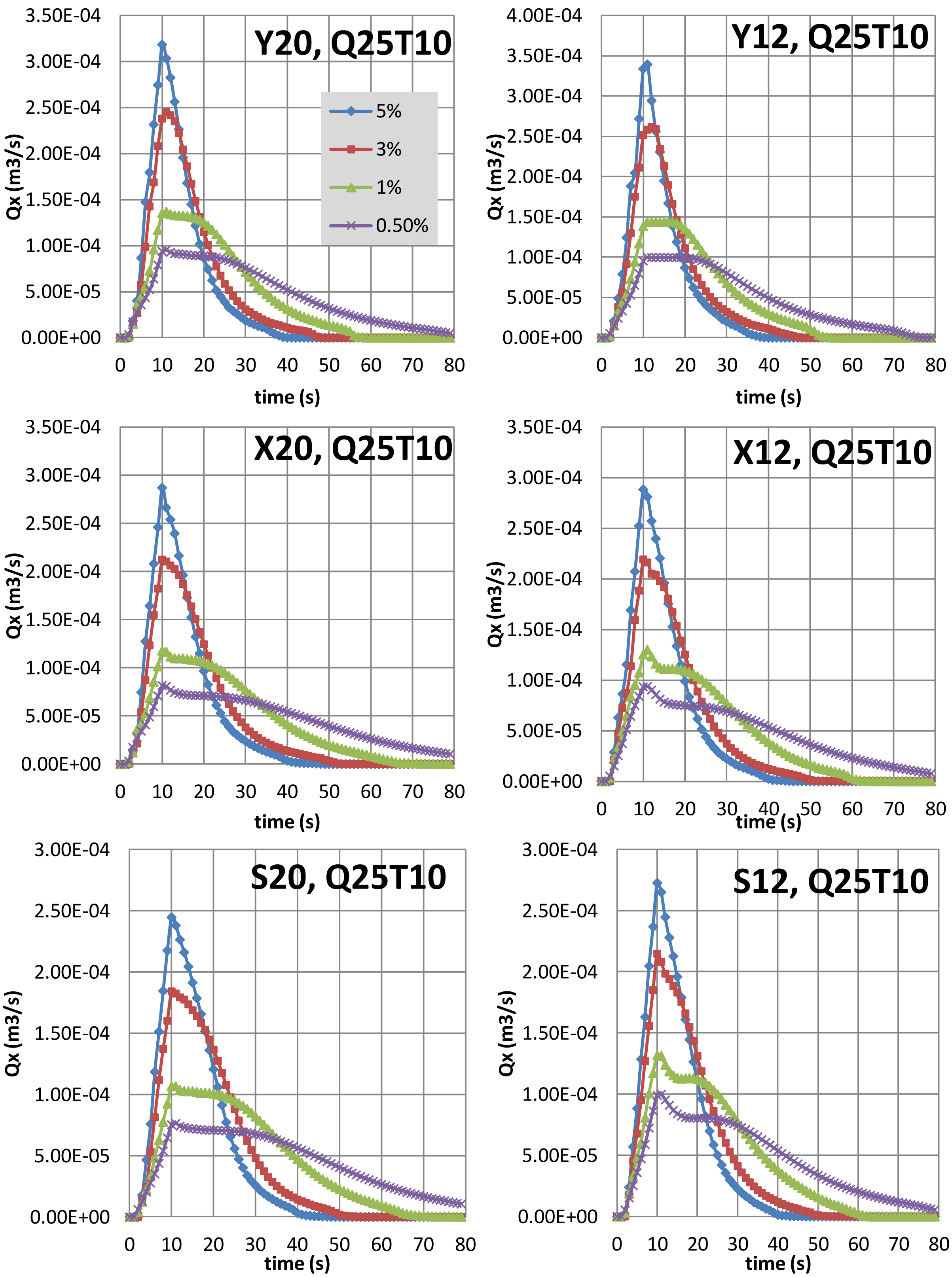

Figure 31(top:a,b; middle: c,d; bottom: e,f)*: Influences of the slope for Y20, Y12, X20, X12, S20 and S12 layouts with Q25T10 hyetograph*

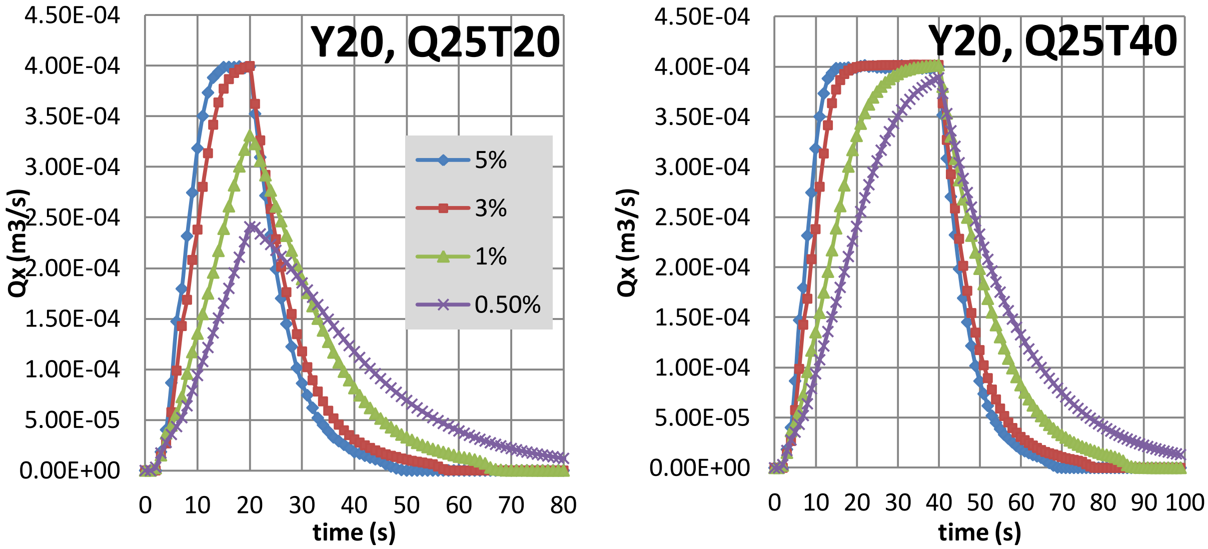

Figure 32(a,b): *Influences of the slope for Y20 layout under Q25T20 and Q25T40 respectively*

4.4.3 Discussion on effects of slope

4.4.3.1 General water depth

Firstly, an increase in slope from 0.5% to 5% causes an increase in the peak discharge and rate of increase of discharge initially. This is observed for all 6 layouts in Figure 31. The rate of reduction in discharge also decreases with decreasing slope as indicated by the falling curve of the hydrographs. This means that water remains in the domain for a longer time when the slope is small which could results in general flooding in real life scenarios if proper drainage systems are not present to remove the rainwater efficiently. Figure 33 shows the water depth profile at t=20s for each of the 4 slopes when layout Y20 is subjected to Q25T10 rainfall. The maximum water depths are 0.017 and 0.0005m for slopes of 0.5% and 5% respectively. Water depths in the domain are also generally higher for slopes of 0.5% as compared to domains with slopes of 5%. The higher water depth shows the slower dissipation of water from the domain when the slope is small.

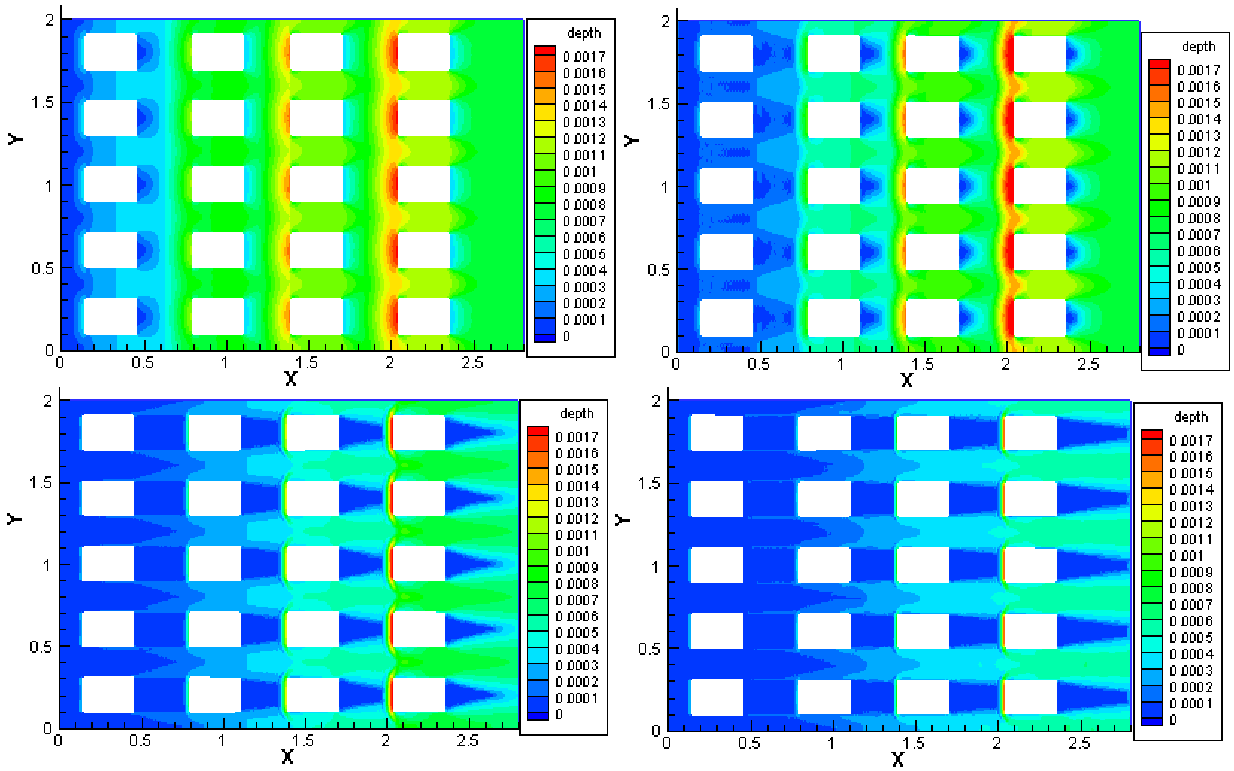

***Figure 33(top:a,b; bottom:c,d)**: Water depth distributions with Y20 and Q25T10 at t = 20s for 0.5%, 1%, 3% and 5% slopes respectively*

<u>4.4.3.2 Localised water depth</u>

In addition, localised flooding may occur when the slopes are higher as water travels down the slope quickly. Figure 34 shows the water depth at the time of peak discharge for each of the 4 slopes. High water depths of 0.0038m are observed near the system outlet when the slope is 5% as water from the top end of the domain rushes down to the outlet. In comparison, the water depth near the outlet when the slope is 0.5% is only 0.0014m approximately.

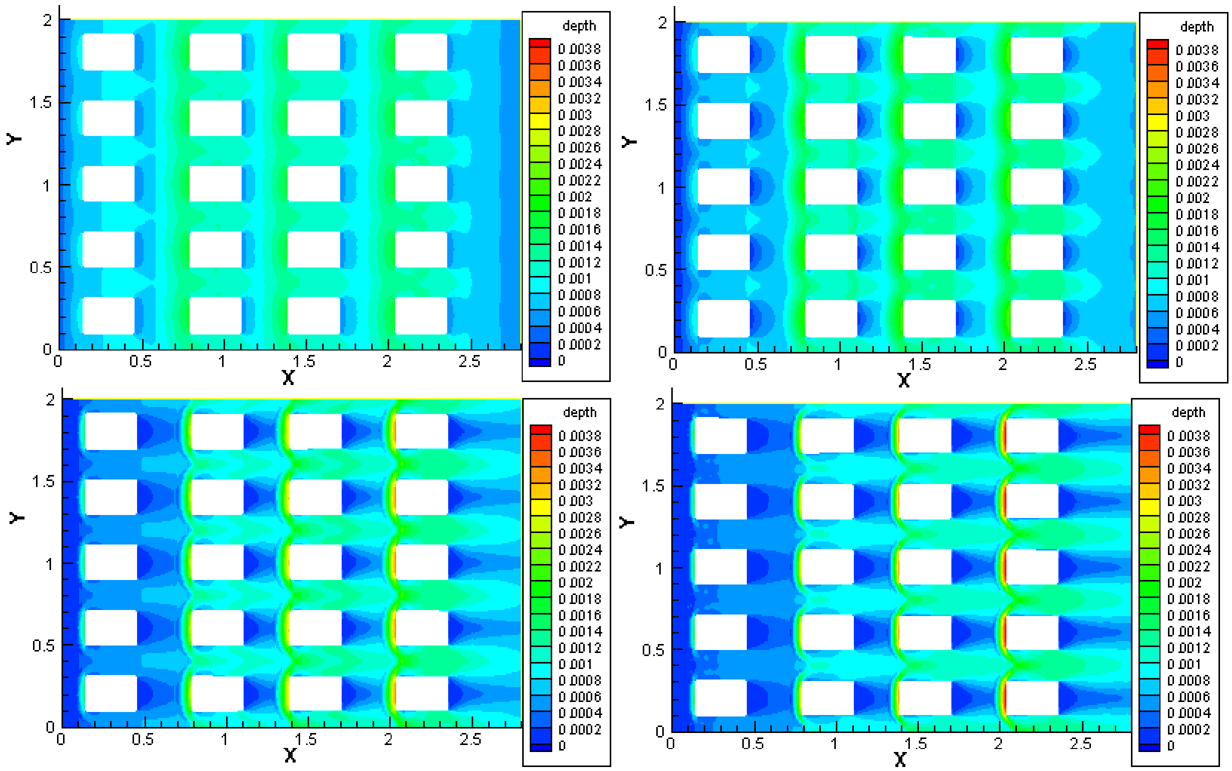

***Figure 34(top: a,b; bottom: c,d)**: Water depth distributions with Y20 and Q25T10 at t = 10s for 0.5%, 1%, 3% and 5% slopes respectively*

<u>4.4.3.3 Water velocity</u>

A third consideration is the velocity of the flow. As expected, the flow velocity is greatest with the larger slopes. Figure 35 shows the velocity (m/s) profile in the domain during peak discharge for each of the 4 slopes with layout Y20 under the Q25T10 hyetograph. For example, a 5% slope produces a peak velocity of 0.28m/s while a 0.5% slope produces a peak velocity of 0.08m/s. The high velocities associated with large slopes highlight the possibility of high velocity flows that may be destructive in extreme cases with highly steep slopes and high intensity rainfall. An example of this is in hillside dwellings during monsoon periods. This can be studied using the numerical model and remedies can be put in place if they are found to be required.

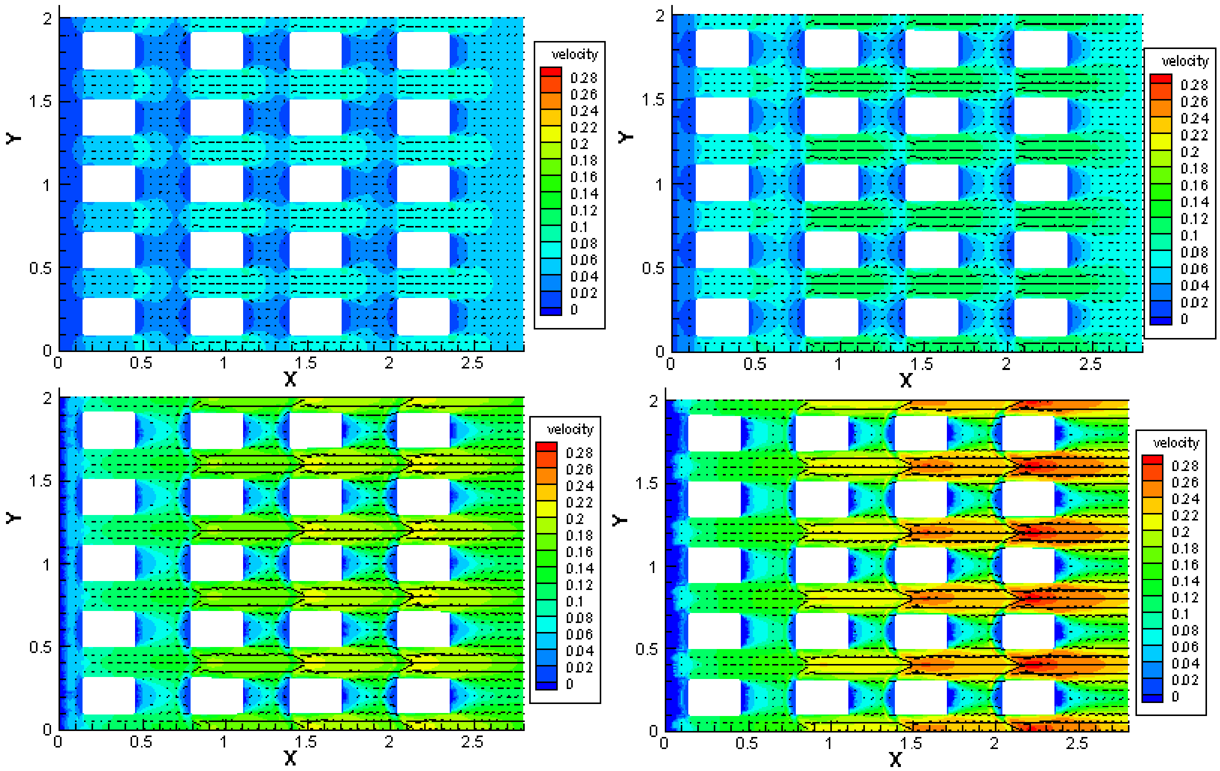

***Figure 35(top: a,b; bottom: c,d)**: Velocity fields with Y20 and Q25T10 at t = 10s for 0.5%, 1%, 3% and 5% slopes respectively*

4.4.3.4 Effects of increased rainfall duration, Q25T20, Q25T40

Further simulations involving the Y20 layout imposed with 25 l/min of rainfall for 20 and 40s were carried out to investigate if the volume of rainfall has implications on the influence of the slopes. The longer durations also allow steady state discharge to be achieved and any differences from the different slopes to be observed. The resulting hydrographs are shown in Figure 32.

In general, the trend of greater rate of increase of discharge and shorter time of concentration with larger slope is still observed. The time of concentration or peak discharge for slopes of 5%, 3%, 1% and 0.5% are 17.5s, 22.5s, 37.5s and 40s respectively. Steady state discharge was not achieved for the simulation involving the slope of 0.5% as the duration of the rainfall was too short. However, the peak discharges for the 3 remaining slopes remain the same and this is expected as an equal amount of water is discharged as is input into the domain during steady state. Discharges across all slopes fall once the rainfall is stopped. In addition, the slower rise in discharge for the lower slopes is due to water being contained in the domain and these are released subsequently resulting in the gentler sloping falling limb.

Overall, these simulations enable the influence of slopes on surface runoff to be studied. In future applications, it is possible to study the rainfall-runoff characteristics associated with a particular combination of slope and layout to model an actual location. Combination of slopes such as that presented in Iwagaki (1955) can also be considered.

4.5 Comparison between building densities

4.5.1 Simulations and output hydrographs

The third factor considered in this study is the building density. 2 building densities involving 20 and 12 buildings were considered for each of the Y, X and S layout. The 6 layouts were subjected to rainfall discharges of 7, 15 and 25 l/min for 10 and 20s, producing a total of 36 simulations. In addition, 6 simulations were carried out with the Q25T40 hyetograph to investigate the effects at steady state. In most cases involving input discharges of 7 and 15 l/min, the differences in density had been insignificant and the results have not been presented. For cases involving input discharge of 25 l/min, Figure 36 show the hydrographs obtained for a rainfall duration of 20s. In addition, the hydrographs produced from the 6 layouts on slopes of 5%, 5%, 3% and 1% with rainfall duration of 10s, 40s, 40s and 60s respectively are shown in Figures 27 to 30 above.

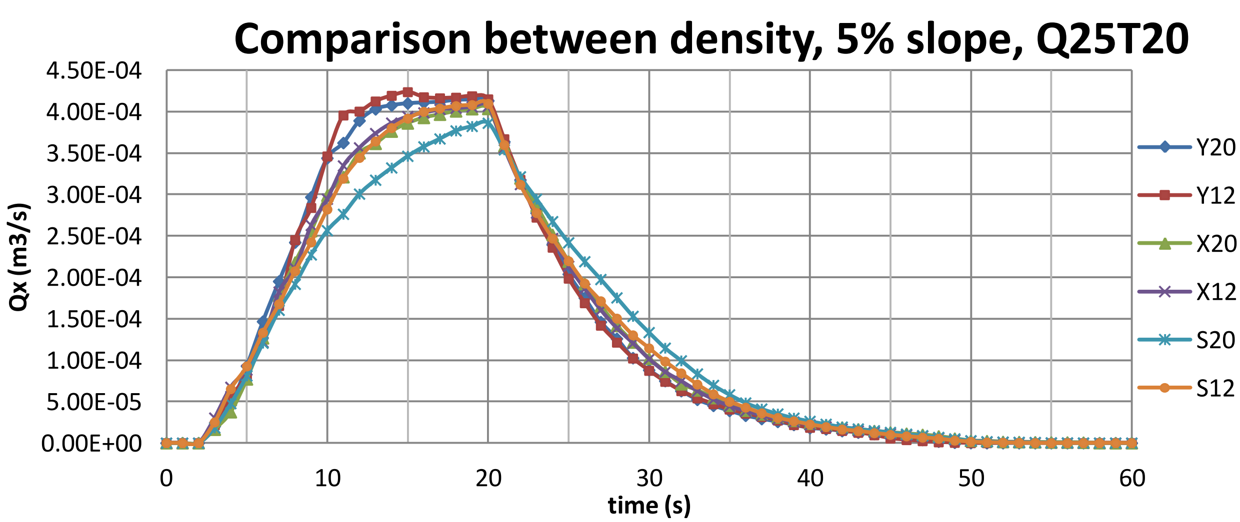

Figure 36: *Comparison between density with 5% slope and Q25T20*

4.5.2 Discussion

In general, the lower the building density, the larger the peak flow. For example, layout Y12 subjected to 25 l/min of rainfall for 10s produced a peak discharge of $3.39 x 10^{-4} m^3/s$. Layout Y20 however produces a smaller peak discharge of $3.18 x 10^{-4} m^3/s$ under the same rainfall. Table 7 shows a summary of the time of peak discharges or concentration and maximum discharges for each of the 6 layouts when subjected to input discharges of 25 l/min for 10, 20 and 40s.

***Table 7**: Summary of time of peak discharge or concentration and maximum discharges, Q25T10, Q25T20, Q25T40*

Layout	Q25T10		Q25T20		Q25T40	
	Time of peak discharge t_p (s)	Peak discharge (m^3/s)	Time of concentration t_c (s)	Peak discharge (m^3/s)	Time of concentration t_c (s)	Peak discharge (m^3/s)
Y20	10.0	3.18×10^{-4}	17.0	4.14×10^{-4}	17.0	4.14×10^{-4}
Y12	11.0	3.39×10^{-4}	14.0	4.17×10^{-4}	14.0	4.17×10^{-4}
X20	10.0	2.87×10^{-4}	20.0	4.03×10^{-4}	23.0	4.05×10^{-4}
X12	10.0	2.88×10^{-4}	20.0	4.07×10^{-4}	20.0	4.07×10^{-4}
S20	10.0	2.45×10^{-4}	20.0	3.86×10^{-4}	25.0	3.94×10^{-4}
S12	10.0	2.73×10^{-4}	20.0	4.09×10^{-4}	21.0	4.11×10^{-4}

The rate of increase and decrease on the rising and falling limb respectively are also faster with a lower building density. This results in a shorter time of concentration and peak flow is expected to occur more quickly for layouts with lower densities. This is shown in Table 7. For example, the time of concentration for layout S12 and S20 under Q25T40 rainfall are 21s and 25s respectively.

However, the layout or rainfall intensity also affects the significance of the differences caused by building density. For example, density makes a significant difference in peak discharges for the S layout with a difference of $0.000028 m^3/s$ between S12 and S20 when the layouts are subjected to 25 l/min of rainfall for 10s as seen in Table 7. For the same rainfall however, negligible difference is observed between the X layouts. Also, lower input discharges of 7 and 15 l/min produced insignificant differences between layouts of different densities. For example, when subjected to 15 l/min of discharge for 10s, layouts X20 and S20 produced largely similar discharges when compared to X12 and S12 respectively. A possible explanation for the similarity in peak discharges is due to the nature in which rainfall is distributed in the domain. Larger rainfall intensities are imposed for X20 and S20 as opposed to X12 and S12 to take into account the different areas occupied by the buildings. This may have an impact on the flow of water in the domain and their contribution to the peak discharge. As the flow pattern is different for each of the layout, the effect may be more significant for the X and S layouts that have more complicated flow patterns. Hence, the general trend remains for the Y layouts with Y12 having a larger peak discharge than Y20. The hydrographs are shown in Figure 26.

In general, differences in density are expected to affect the surface runoff characteristics. As only 2 densities and a number of input hyetographs based on models by Cea et al. (2009) had been considered in this study, the significance of density is less obvious and future studies could consider more combinations of building densities and input rainfall.

4.6 Other features-Localised flow pattern

The effects of building layouts, terrain slopes and building densities on the surface runoff in urban settings were investigated in the previous 3 sections. In addition, other features can also be studied from the numerical simulation. These include the flow patterns related to the different layouts, the localized water velocity and water depth. These are important as extreme cases of localized high velocity or water depth may results in localized flooding, pooling of water, erosion or structural failure. Understanding where these features occur and their magnitude would hence provide opportunities for remediating these problems. Figure 37 shows the distribution of water depth and velocity for the S12 layout under a Q25T10 hyetograph at the time of peak discharge. The complicated building layout associated with the S12 layout result in a complicated flow pattern and high water depths locally around building which may be a problem in real life scenarios.

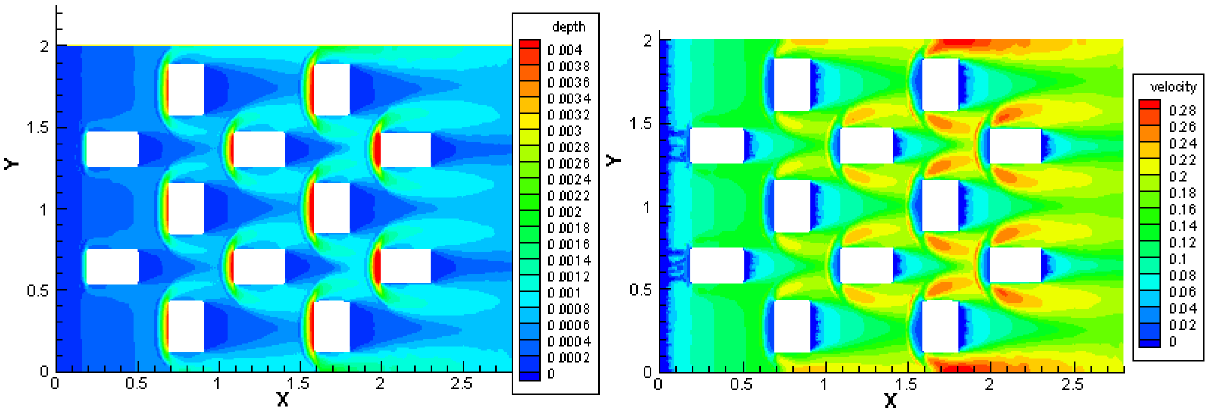

***Figure 37(a,b)**: Water depth and velocity distributions with S12 and Q25T10 at t = 10s*

5. Conclusions

The relationship between rainfall and runoff in an urban environment was studied using an in-house computer model based on the TVD-MacCormack scheme. The influence of buildings that act as obstructions in the flow of surface runoff from direct precipitation were studied by considering factors including the layout of the buildings, the terrain slope and the density of the buildings.

The numerical model used was validated by reproducing 1D and 2D analytical results and experiments conducted by Iwagaki (1955), Gottardi & Venutelli (2008), Cea et al. (2008) and Cea et al. (2009). Simulations on 1D flow based on experimental results by Iwagaki (1955) indicated the need to calibrate the Manning's roughness coefficient accurately. The overall shapes of the hydrographs were well-predicted but the simulation overestimated the peak discharge, indicating that a larger value of Manning's coefficient was required. 1D simulations were also carried out based on hypothetical, analytical and experimental cases presented in Gottardi & Venutelli (2008). Simulation results compared very well with the published results, with slight errors indicating the possibility of problems when simulating very small slopes. 2D simulations involved replicating physical experiments by Cea et al. (2008) and Cea et al. (2009) that were based on obstructions on a 3-slope terrain. Validation tests based on Cea et al. (2009) enabled 3 methods of representing buildings to be compared. The Building-Hole method in which buildings were represented as holes in the numerical mesh was chosen for subsequent simulations. The Manning's coefficient was also set as $0.01m^{-1/3}s$ and it was found that the numerical domain had to be extended to generate rapid flows at the downstream boundary, so as to reproduce the effect of the sudden ground level decrease at the catchment outlet in physical experiments. The importance of defining the topography of the domain accurately was also noted.

The numerical model was then applied for parametric study with building layouts and rainfall hyetographs based on Cea et al. (2009).

Layout was found to influence the surface runoff. In general, the discharges were largest when buildings were aligned with their length parallel to the direction of the water flow. Complicated layouts with staggered arrangement of buildings provide greater obstruction and reduce the rate of discharge out of the domain. Build-up of water could hence occur in the domain and represent flooding in urban areas in real scenarios. Potential problems in the simulations associated with steep slopes and rapid flows such as discrepancies in peak discharges between the different layouts were noted from simulations involving 5% slopes and Q25T40. These issues should be considered in future simulations. Lastly, the influence of layout is affected by factors such as the rainfall intensity. For example, the relationship between the layouts mentioned above is less significant when discharges of 7 and 15 l/min were imposed. The difference between the peak discharges for the X and S layouts were insignificant while that produced by the Y layouts were significantly larger when 15 l/min of discharge were imposed for 10s.

Terrain slope of 0.5%, 1%, 3% and 5% were considered. Generally, larger slopes produced hydrographs with shorter time of concentration and larger peak discharges. Issues of flooding could occur with both steep and gentle slopes. For example, general flooding could occur with smaller slopes as water dissipates slowly and remain in the domain for longer periods of time. On the other hand, localised flooding could occur in regions near the domain outlet when the slopes are large as water flow down the slopes rapidly and collect at the system outlet. A third consideration is the flow velocity, with larger slopes producing greater flow velocities. In extreme cases, these flows could be destructive and can be modelled using the numerical model.

Lastly, lower building density was found to reduce the time of concentration and increase the peak discharge. Its significance was however influence by the layout and rainfall intensity imposed. For example, a significant difference in peak discharges exists between S12 and S20 when the layouts are subjected to 25 l/min of rainfall for 10s. For the same rainfall however, negligible difference is observed between the X layouts. Also negligible differences are observed when 7 or 15 l/min of discharge are imposed.

The simulations carried out have shown the capability and potential of the numerical model in modelling surface runoff in urban areas due to a direct input of precipitation on the area. Although the simulations carried out have involved simplified and hypothetical representation of buildings and slopes, they provide a strong foundation for understanding how building layout, slope and building density may affect the surface runoff characteristics.

These simulations can be further developed by considering a larger range of factors such as different building layouts, slopes, building densities, building shapes, rainfall intensities and surface roughness. The results from a collection of such simulations can be combined to obtain the surface runoff characteristics for a larger development consisting of a number of terrains of different slopes, building or surface features. This would provide a useful tool for the design of new urban developments and their drainage systems.

Existing urban developments contain features such as road, drains, sewers and parks that would affect the surface runoff. These are not considered in the existing model. However, future development in numerical studies could include such features, providing an opportunity for highly accurate studies of real developments and even real-time simulation of surface runoff during precipitation events.

6. References

Cea L, Puertas J, Pena L, Garrido M, 2008. Hyrdrological forecasting of fast flood events in small catchments with a 2D-SWE model. Numerical model and experimental validation. In: World Water Congress 2008, 1-4 September 2008, Montpellier, France.

Cea L, Garrido M, Puertas J, 2009. Experimental validation of two-dimensional depth-averaged models for forecasting rainfall-runoff from precipitation data in urban areas. Journal of Hydrology 2010; 382:88-102

Fiedler FR, Ramirez JA, 2000. A numerical method for simulating discontinuous shallow flow over an infiltrating surface. International Journal for Numerical Methods in Fluids; 32: 219-240

Gottardi G, Venutelli M (2008). An accurate time integration method for simplified overland flow models, Advances in Water Resources 2008; 31(1): 173-180

Govindaraju RS, Kavvas ML, Jones SE, 1990. Approximate analytical solutions for overland flows. Water Resource Res 1990; 26(12): 2903-2912

Iwagaki Y, 1955. Fundamental studies on the runoff analysis by characteristics. Bulletins-Disaster Prevention Research Institute, Kyoto University 1955, 10: 1-25.

Liang D, Falconer RA, Lin B, 2006. Simulation of rapidly varying flow using an efficient TVD-MacCormack scheme. International Journal for Numerical Methods in Fluids 2007; 53:811-826

Morgali JR, Linsley RK, 1965. Computer analysis of overland flow. Journal of the Hydraulics Division – ASCE 1965; 91(3): 81-100

Schubert JE, Sanders BF, Smith MJ, Wright NG, 2008. Unstructured mesh generation and landcover-based resistance for hydrodynamic modelling of urban flooding. Adv. Water Resour.

United Nations, Department of Economic and Social Affairs, Population Division (2012). World Urbanization Prospects: The 2011 Revision, CD-ROM Edition

Appendix 1: Risk Assessment Retrospective

The only risks associated with this project were health related risks associated with prolonged use of computing equipment. These included bad posture resulting in neck and back aches and tiredness of eyes from looking at the computer screen for long durations. In retrospect, these risks were highly pertinent but very easily overlooked. More care regarding these risks should be taken when completing similar projects in the future.